



**PROCESS MODELING OF WASTE HEAT
RECOVERY SYSTEMS TO GENERATE POWER
IN FALLUJAH WHITE CEMENT PLANT**

**2021
MASTER THESIS
MECHANICAL ENGINEERING**

Hussein Ali MUTLAG

Assist. Prof. Dr. Abdulrazzak AKROOT

**PROCESS MODELING OF WASTE HEAT RECOVERY SYSTEMS TO
GENERATE POWER IN FALLUJAH WHITE CEMENT PLANT**

Hussein Ali MUTLAG

**T.C.
Karabük University
Institute of Graduate Programs
Department of Mechanical Engineering
Prepared as
Master Thesis**

**Thesis Advisor
Assist. Prof. Dr. Abdulrazzak AKROOT**

**KARABÜK
November 2021**

I certify that in my opinion the thesis submitted by Hussein Ali MUTLAG titled “PROCESS MODELING OF WASTE HEAT RECOVERY SYSTEMS TO GENERATE POWER IN FALLUJAH WHITE CEMENT PLANT ” is fully adequate in scope and in quality as a thesis for the degree of Master of Science.

Assist. Prof. Dr. Abdulrazzak AKROOT
Thesis Advisor, Department of Mechanical Engineering

This thesis is accepted by the examining committee with a unanimous vote in the Department of Mechanical Engineering as a Master of Science thesis. 04/11/2021

<u>Examining Committee Members (Institutions)</u>	<u>Signature</u>
Chairman : Assist. Prof. Dr. Erhan KAYABAŞI (KBU)
Member : Assist. Prof. Dr. Abdulrazzak AKROOT (KBU)
Member : Assist. Prof. Dr. Fatih Uysal (SUBU)

The degree of Master of Science by the thesis submitted is approved by the Administrative Board of the Institute of Graduate Programs, Karabük University.

Prof. Dr. Hasan SOLMAZ
Director of the Institute of Graduate Programs



“I declare that all the information within this thesis has been gathered and presented in accordance with academic regulations and ethical principles and I have according to the requirements of these regulations and principles cited all those which do not originate in this work as well.”

Hussein Ali MUTLAG

ABSTRACT

M. Sc. Thesis

PROCESS MODELING OF WASTE HEAT RECOVERY SYSTEMS TO GENERATE POWER IN FALLUJAH WHITE CEMENT PLANT

Hussein Ali MUTLAG

Karabük University

Institute of Graduate Programs

The Department of Mechanical Engineering

Thesis Advisor:

Assist. Prof. Dr. Abdulrazzak AKROOT

November 2021, 78 pages

Cement manufacturing is an energy-intensive industry with energy typically comprising 40-50% of production costs. Cogeneration cycles are used in cement plants to recover waste heat from clinker cooler exhaust and the preheater exhaust gases to reduce the power needed to produce cement in addition to lowering carbon dioxide emissions. This study analyzes the thermal energy used in the cement industry, which is one of the most heat-consuming industries. Opportunities to recover waste heat in this industry are an important target. The main source of energy for a cement manufacturing plant is heavy fuel oil, which accounts for approximately 94% of the thermal energy used in the cement industry. The study conducted on the White Cement Factory in Fallujah showed that the plant consumed approximately 50% of the heat sources to produce the clinker and the remaining part was lost to the environment without benefit from it through the exhaust gases from reheating and the clinker grille air cooler. The basics of the waste heat recovery project are the air quenching cooler

(AQC), suspension preheater (SP), and cogeneration cycles such as the organic Rankine cycle, a single steam flash cycle, and a dual pressure steam cycle. Energy and exergy analysis is the most powerful tool for the evaluation of the performance of generating plants for the cycles mentioned above. The results showed that the single steam flash cycle is the best performing cogeneration cycle in power output and thermal and exergy efficiencies. The results also showed that the power produced from the Dual-Pressure steam cycle is 14095 kW at a thermal efficiency of 33.18% and exergy efficiency of 51.17%.

Keywords : Cement industry, Waste Heat Recovery, air cooled chiller (AQC), Suspension preheater (SP), Cogeneration cycles.

Science Code: 91408

ÖZET

Yüksek Lisans Tezi

FELLUCE BEYAZ ÇİMENTO FABRİKASI ATIK ISI GERİ KAZANIM DÖNGÜSÜ VE GÜÇ ÜRETİM SİSTEMİ PROSES MODELLEMESİ

Hussein Ali MUTLAG

Karabük Üniversitesi

Lisansüstü Eğitim Enstitüsü

Makina Mühendisliği Anabilim Dalı

Tez Danışmanı:

Asst. Prof. Dr. Abdulrazzak AKROOT

Kasım 2021, 78 sayfa

Çimento üretimi, enerjinin tipik olarak üretim maliyetlerinin %40-%50'sini oluşturduğu enerji yoğun bir endüstridir. Kojenerasyon çevrimleri, çimento fabrikalarında, klinker soğutucu egzozundan ve ön ısıtıcı egzoz gazlarından atık ısıyı geri kazanmak ve çimento üretmek için gereken gücü azaltmak ve karbondioksit emisyonlarını düşürmek için kullanılır. Bu çalışma, yüksek miktarda ısı tüketen çimento endüstrisinde kullanılan termal enerjiyi analiz etmektedir. Bu endüstride atık ısıyı geri kazanma potansiyelinin araştırılması önemli bir hedefdir. Bir çimento üretim tesisi için ana enerji kaynağı, çimento endüstrisinde kullanılan termal enerjinin yaklaşık %94'ünü oluşturan ağır akaryakıttır. Felluce'deki Beyaz Çimento Fabrikası'nda yapılan çalışma, fabrikanın klinker üretmek için ısı kaynaklarının yaklaşık %50'sini tükettiğini ve kalan kısmının ise yeniden ısıtmadan çıkan egzoz gazları ve klinker ızgara havası yoluyla kullanılmadan çevreye atıldığını göstermiştir.

Atık ısı geri kazanım projesinin temelleri, hava söndürmeli soğutucu (AQC), süspansiyonlu ön ısıtıcı (SP) ve organik Rankine çevrimi, tek bir buhar flaş çevrimi ve bir çift basınçlı buhar çevrimi gibi kojenerasyon çevrimleridir. Enerji ve ekserji analizi, yukarıda bahsedilen çevrimler için üretim tesislerinin performansının değerlendirilmesi için en güçlü araçtır. Sonuçlar, tek buharlı flaş çevriminin, güç çıkışı ve termal ve ekserji verimliliğinde en iyi performansı kojenerasyon çevriminin gösterdiği ortaya çıkmıştır. Sonuç olarak, bir çift basınçlı buhar çevriminden %33.18 ısıl verimlilikte ve %51.17 ekserji verimliliğinde 14095 kW güç üretimi gerçekleştirilebileceği hesaplanmıştır.

Anahtar Kelimeler : Atık Isı Geri Kazanımı, Kazanlar, Enerji, Çimento Fabrikası, Rankine Çevrimi, Teps

Bilim Kodu : 91408

ACKNOWLEDGMENT

I dedicate this humble effort to my father and mother, and my family who always stood by my side and supported me through my studies and beyond. I will always be in debt for them and may Allah (SWT) grant me the power to show my appreciation and gratitude to them. Moreover, I would humbly dedicate this work to my supervisor, Assist. Prof. Dr. Abdulrazzak AKROOT who has guided me and supported through the roughest of times and without her I would not be able to achieve this status and finish this research. Furthermore, I would like to show my appreciation to all of the hardworking lecturers and staff members of the faculty of engineering faculty at Karabuk University.

CONTENTS

	<u>Page</u>
APPROVAL.....	ii
ABSTRACT.....	iv
ÖZET.....	vi
ACKNOWLEDGMENT.....	viii
CONTENTS.....	ix
LIST OF FIGURES	xii
LIST OF TABLES	xiv
SYMBOLS AND ABBREVIATIONS	xv
PART 1	1
INTRODUCTION	1
1.1. BACKGROUND.....	1
1.2. ENERGY USE IN THE CEMENT INDUSTRY.....	3
1.3. SCENARIO OF COGENERATION IN OTHER COUNTRIES.....	5
1.4. ENERGY MANAGEMENT METHODS BEING PROMOTED	6
1.4.1. Improvements to the Equipment	6
1.4.2. Improvement of the Process	6
1.5. AVAILABILITY OF WASTE HEAT	7
1.5.1. Waste Heat Recovery and Power Generation	7
1.5.2. Advantages of WHR in Cement Plants	8
1.5.3. Cogeneration Possibilities	9
1.5.4. TYPES OF WASTE HEAT RECOVERY APPLICATIONS	10
1.5.4.1. Standard Rankine Cycle.....	10
1.5.4.2. Rankine Organic Cycle.....	11
1.5.4.3. The Kalina Cycle	12
1.6. WASTE HEAT BOILER LOCATION.....	14
1.6.1. Appropriateness of the WHR Boiler	15
1.6.2. Maximum Temperature of Flue Gas	16

	<u>Page</u>
1.6.3. Summary.....	16
1.7. RESEARCH GOALS AND MOTIVES	17
1.8. STUDY OVERVIEW	18
PART 2	20
LITERATURE REVIEW.....	20
2.1. RESEARCH PROBLEMS	39
PART 3	41
METHODOLOGY.....	41
3.1. THERMODYNAMIC ANALYSIS AND SIMULATION SCHEME FOR ORGANIC RANKINE CYCLE.....	41
3.1.1. Pump Parameter.....	42
3.1.2. Turbine Parameter	43
3.2.3. Condenser Parameter.....	43
3.1.4. Mixer Parameter	44
3.1.5. Separatore Parameter.....	44
3.1.6. AQC Boiler Parameter	44
3.1.7. SP Boiler Parameter	45
3.1.8. Drum.....	47
3.1.9. ORC Performance	47
3.2. THERMODYNAMIC ANALYSIS AND SIMULATION SCHEME FOR STEAM CYCLE WITH SINGLE FLASH	47
3.2.1. Pumps Parameter	48
3.2.2. Turbines Parameter.....	49
3.2.3. Condenser Parameter.....	49
3.2.4. Flasher Parameter	50
3.2.5. Mixers Parameter.....	50
3.2.6. Separator Parameter.....	51
3.2.7. Valve Parameters.....	52
3.2.8. AQC Boiler Parameter	52
3.2.9. SP Boiler Parameter	52

	<u>Page</u>
3.2.10. Single Flash Cycle Performance	53
3.3. THERMODYNAMIC ANALYSIS AND SIMULATION SCHEME FOR STEAM CYCLE WITH DUAL PRESSURE	53
3.3.1. Pumps Parameter	54
3.3.2. Turbines Parameter.....	55
3.3.3. Condenser Parameter.....	56
3.3.4. Mixers Parameter.....	56
3.3.5. AQC Boiler Parameter	57
3.3.6. SP Boiler Parameter	57
3.3.7. Dual Steam Cycle Performance.....	57
3.4. COGENERATION SYSTEMS INPUT PARAMETER.....	58
PART 4	59
RESULTS	59
PART 5	70
CONCLUSION AND RECOMMENDATIONS.....	70
5.1. CONCLUSION	70
5.2. RECOMMENDATIONS	71
REFERENCES.....	72
RESUME	78

LIST OF FIGURES

	<u>Page</u>
Figure 1.1. Fallujah White Cement Plant.....	2
Figure 1.2. Cement production and power generation from WHR.....	3
Figure 1.3. Average world-specific energy consumption.....	4
Figure 1.4. Main manufacturing sub-processes receive material and energy flows .	5
Figure 1.5. Waste heat sub-process availability on a regular basis.....	7
Figure 1.6. Power generation from waste heat recovery.....	8
Figure 1.7. Cement kiln heat balance and heat utilization potential	10
Figure 1.8. Standard Rankine cycle in a cement plant.....	11
Figure 1.9. Organic Rankine cycle in a cement plant	12
Figure 1.10. Layout of the Kalina cycle in the cement plant	13
Figure 1.11. Waste heat boilers located in cement plants.....	15
Figure 1.12. WHR framework overview	17
Figure 2.1. Distribution of WHR in rotary kiln	21
Figure 2.2. Reduced emission oxygen kiln process	22
Figure 2.3. Rotary kiln procedure	23
Figure 2.4. General pre-processing in a cement manufacturing plant	24
Figure 2.5. WHR system of a typical cement factory	25
Figure 2.6. Typical scheme of production operations in a cement facility	26
Figure 2.7. (A) Rotary kiln; (b) Temperature distribution of the kiln shell as shown by thermal imaging	27
Figure 2.8. Diagram of the simulation process	28
Figure 2.9. Diagram of Yazd combined-cycle generating station	29
Figure 2.10. ORC with condensate in direct contact	30
Figure 2.11. A phase of hybrid heat recovery	30
Figure 2.12. Three-level hierarchical structure of the bottom-up model.....	31
Figure 2.13. Primary flow sheet of the cement manufacturing process.....	32
Figure 2.14. ORC flow diagram.....	33

	<u>Page</u>
Figure 2.15. Manufacturing clinker	34
Figure 2.16. Method of using a dry kiln.	35
Figure 2.17. Diagram of the system analyzed by Naeimi et al. (2019).....	35
Figure 2.18. WHR in a cement plant by basic ORC	36
Figure 2.19. Heat absorption diagram around the kiln.....	37
Figure 2.20. Heat absorber components around the kiln	38
Figure 2.21. In the cement industry, WHR is idealized for electricity generation using the Kalina cycle	39
Figure 3.1. Organic Rankine cycle at the cement plant.	42
Figure 3.2. Steam cycle with a single flash.....	48
Figure 3.3. Dual steam cycle at the cement plant.	54
Figure 4.1. The (T-S) diagram for ORC.	61
Figure 4.2. Exergy loss given exergy input percentages by ORC.	62
Figure 4.3. The (T-S) diagram for single flash cycle.....	65
Figure 4.4. Exergy loss given exergy input percentages by single flash cycle.....	66
Figure 4.5. The (T-S) diagram for Dual-pressure steam cycle.	68
Figure 4.6. Exergy loss given exergy input percentages via dual steam cycle.....	69

LIST OF TABLES

	<u>Page</u>
Table 3.1. Input parameter for cogeneration systems	58
Table 4.1. Main parameters of pre-heating at the Fallujah White Cement Plant.....	59
Table 4.2. Conditions of exhaust gases for the Fallujah cement plant.....	59
Table 4.3. Main assumptions for the system.....	60
Table 4.4. ORC Performance.	60
Table 4.5. The properties for each state for the organic Rankine cycle.....	61
Table 4.6. ORC exergy input, output and losses.....	62
Table 4.7. Single flash cycle performance.....	63
Table 4.8. The properties for each state for the single flash steam cycle.	64
Table 4.9. Signal flash cycle exergy input, output, and losses.....	65
Table 4.10. Dual-Pressure steam performance.	67
Table 4.11. The properties for each state for the dual-pressure steam cycle	67
Table 4.12. Dual-pressure steam exergy input, output, and losses.	68
Table 4.13. Results of improvement for various cogeneration systems.	69

SYMBOLS AND ABBREVIATIONS

SYMBOLS

T_0	Environment Temperature [$^{\circ}\text{C}$]
P_0	Atmospheric Pressure [MPa]
\dot{m}	The mass flow rate [KG/s]
P	The pump
h	The enthalpy [kJ/kg]
S	The entropy [kJ/Kg.K]
EX	The exergy
Ed	The exergy destroyed
η	The efficiency
\dot{Q}	Heat flow rate [kW]
\dot{Q}_{AQC}	Heat flow rate at AQC boiler [kW]
\dot{Q}_{SP}	Heat flow rate at SP boiler [kW]
$h_{in,air}$	Enthalpy of air at inlet [KJ/kg]
$h_{out,air}$	Enthalpy of air at outlet [KJ/kg]
$h_{in,gas}$	Enthalpy of exhaust gases at inlet [KJ/kg]
$h_{out,gas}$	Enthalpy of exhaust gases at outlet [KJ/kg]
$\dot{m}_{ex,g}$	Mass flow rate of exhaust gases at outlet [kg/s]
$T_{in,ex,g}$	Temperature of exhaust gases at inlet [$^{\circ}\text{C}$]
$T_{out,ex,g}$	Temperature of exhaust gases at outlet [$^{\circ}\text{C}$]
\dot{W}	Power output [kW]
η_{th}	Thermal efficiency
η_{EX}	Exergy efficiency

η_T	Turbine efficiency
η_P	Pump efficiency
\dot{w}_T	Work turbine [kW]
\dot{w}_P	Work pump [kW]
\dot{w}_{net}	Net produced work [kW]
Ed_p	Exergy destroyed for pump [kW]
Ed_T	Exergy destroyed for turbine [kW]
Ed_{Total}	Exergy destroyed Total [kW]
\dot{Q}_{con}	Heat flow rate at condenser [kW]
Ed_{mix}	Exergy destroyed for mixer [kW]
Ed_{flash}	Exergy destroyed for flasher [kW]
Ed_{sep}	Exergy destroyed for separator [kW]

ABBREVIATIONS

WHR	Waste Heat Recovery
AQC	Air Quenched Cooler
EES	Engineering Equations Solver
ORC	Organic Rankine Cycle
SP	Suspension preheater
TEGs	Thermal Electric Generated System
WHRs	Waste Heat Recovery System
Sep	Separator
Mix	Mixer

PART 1

INTRODUCTION

1.1. BACKGROUND

The value of the lost heat recovery project in cement plants lies in the fact that it fosters creativity, discovery, and problem-solving. As shown in Figure 1.1, the cement industry has become a global industry recently as global demand for this product has increased annually from 1.8 billion tons to 3.7 billion tons within ten years [1]. At the same time, the industry is a highly energy-consuming industry, where a thermal energy consumption of more than 75% of primary energy use has been calculated. In other words, up to 2.95 GJ of average energy is consumed to produce one ton of cement in developed kiln types in industrialized countries. This energy consumption may increase to 5 GJ, [1] which attracts the attention of engineers as to how to reuse the energy lost from outside the kiln shell, estimated to be 15% [2]. The exhaust gas temperature ranges from 300°C to 350°C at the beginning of the furnace heating. In addition, the temperature of the clinker produces temperatures of up to 1,000°C. Using flowing air, clinkers cool to between 100°C and 120°C and there is a wasted temperature between 200°C and 300°C. Due to the low temperatures, it is possible to use the Rankine cycle to recover wasted heat from the cement industry. Moreover, emissions into the environment can be reduced and this heat can be utilized to generate electricity. Simultaneously, making the plant a cement producer and an electrical energy producer will attract investors into this industry [3].



Figure 1.1. Fallujah White Cement Plant.

The cement production process causes a loss of heat estimated to be 35-40% through the air currents for cooling the clinker and through the exhaust gases. In addition, there is heat waste with 26% of the energy entering the cement production process through the hot air generators used in furnace heating. In addition to reducing reliance on the national grid, the WHRS reduces the discharge of greenhouse gases, which will help to improve plant performance [4].

In order to take advantage of this heat in generating electrical energy, we recover this energy and return it to the system, as shown in Figure 1.2. This reduces the cost of production. The calculated field of work on two heat sources is the clinker grate air cooler and the reheating tower for raw materials, noting that the heat emitted from these sources is not without contamination of raw materials. In this study, the work will be on a rotary kiln 163 m in length and 3.5 m in diameter, and a rotation speed of 5 rpm [4]. Methods and systems to convert waste heat from cement plants into electrical energy contribute to the cement industry and reduce energy spent on this industry's energy. Two heat sources in the cement plant are used, the first of which consists of a hot air current from the cooling clinker, and second consisting of exhaust gases. The results achieved include electrical power generation. Heavy fuel oil is used

in furnaces and is heated, and the raw materials used in the cement industry are dried [5].

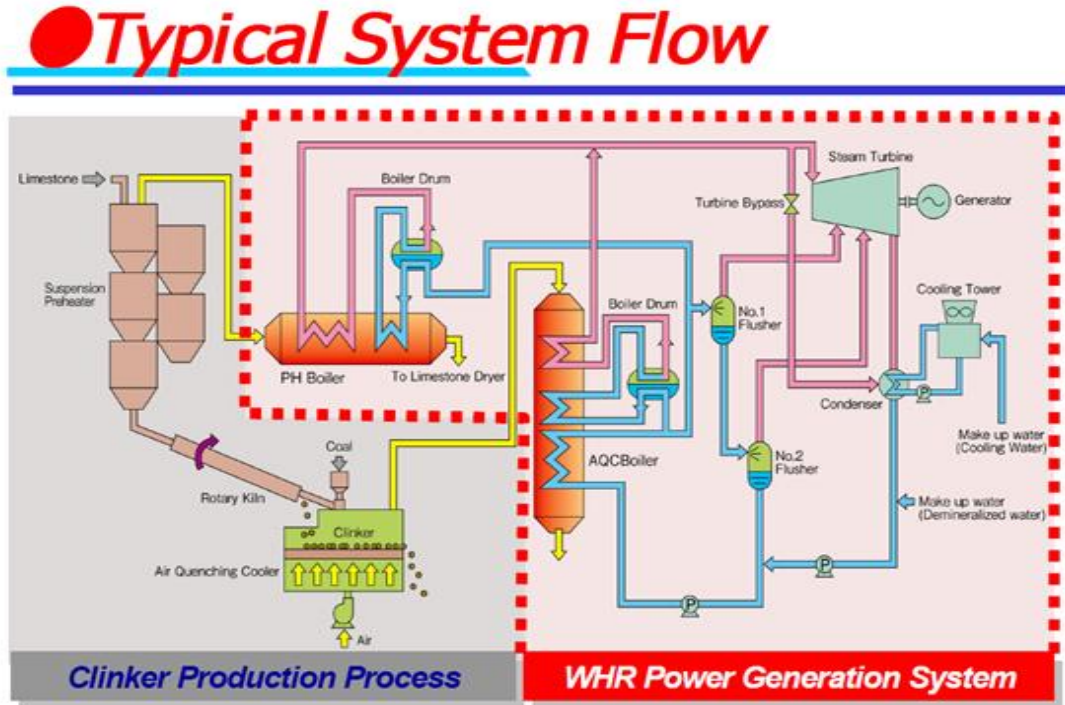


Figure 1.2. Cement production and power generation from WHR [6].

1.2. ENERGY USE IN THE CEMENT INDUSTRY

The cement industry consumes fossil fuels and alternative fuels to burn raw materials inside the kiln and electrical energy in crushing and grinding raw materials and cooling and grinding the clinker. The amount of energy consumed varies according to the approved manufacturing method (wet-dry, preheated, pre-calcined, etc.), the type of fuel used, the ratio of clinker to cement, the kind of furnaces (rotary, coaxial), the efficiency of the equipment used and its technical conditions. The theoretical thermal energy required to manufacture clinker (the main cement component) is estimated at 1.65, as shown in Figure 1.3.

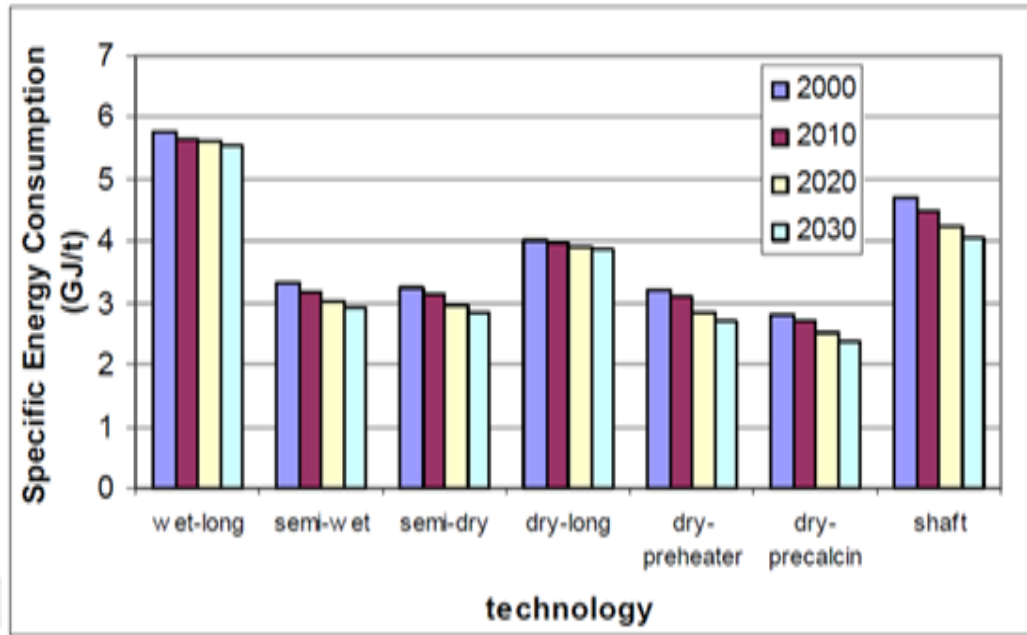


Figure 1.3. Average world-specific energy consumption [7].

The amount of actual heat energy needed is twice that amount, up to 1.20 GJ per ton (2), as losses constitute a significant proportion of the heat energy consumed. There are two ways to produce cement in rotary kilns. The first is the wet method, which is somewhat old, where the average global consumption is 6.3 gigajoules per ton of clinker. In contrast, the average global consumption lies between 3 and 3.5 gigajoules per ton of clinker. The heat energy consumed is distributed in a typical rotary kiln equipped with a four-stage coordinated heater operating in the dry process (20). Those stages are the theoretical heat power required being 50%; thermal energy lost in combustion gases being 22%; lost heat energy in the clinker being 5%, and thermal energy loss through radiation and convection being 12 %. This distribution indicates that there is good potential to improve the thermal efficiency of cement kilns by recovering waste heat and improving thermal insulation [8]. Electrical energy is used in all stages of production. Electrical power consumption has decreased from 150 kilowatt-hour per ton of cement in the 1960s to less than 20 kilowatt-hours per ton of cement today. Consumption in some modern establishments has decreased to approximately 75 kilowatts per ton of cement due to high-efficiency equipment. The electrical energy consumed in the cement industry is generally distributed in percentages [9].

The specific consumption per ton of cement varies from one country to another, with an average energy consumption of 5 GJ per ton in Eastern Europe and the former Soviet Union, 4.5 GJ per ton in North America and 5.1 GJ per ton in the Middle East. Energy efficiency measures have been taken in many cement-producing countries in the previous period. In China, which accounts for approximately 40% of world production, energy consumption has fallen by about 10% (from 5-6 GJ per ton of cement in 1990 to approximately 5 GJ per ton of cement today). In addition, in the United States of America, consumption has fallen by 4% from 1994 to 2000 [10]. Global primary energy consumption has decreased by not less than 5%, i.e., to approximately 4.6 gigajoules per ton of cement, equivalent to 10 kg of oil. Accordingly, the primary energy consumed in cement production is estimated at the global level for the year 2009 to be approximately 8.6 million mega joules equivalent to 200 million tons of oil, representing 3.1% of primary energy consumption and 5% of total energy consumption in the industrial sector worldwide [11]. Figure 1.4 presents the main manufacturing sub-processes that receive material and energy flows.

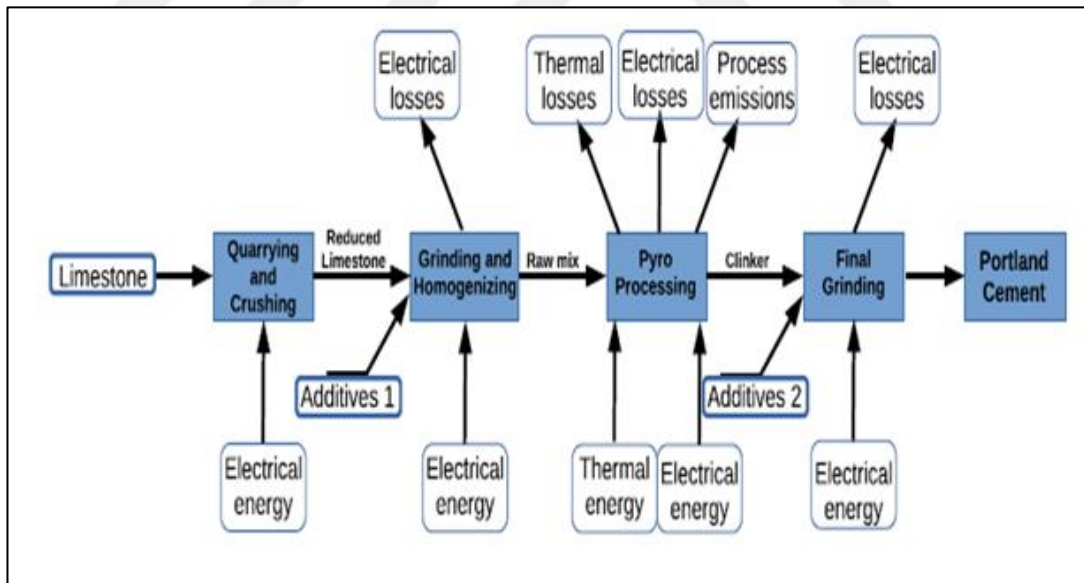


Figure 1.4. Main manufacturing sub-processes receive material and energy flows [12].

1.3. SCENARIO OF COGENERATION IN OTHER COUNTRIES

Both Japan and China took the initiative to develop joint power generation systems in cement factories. Japan ranked first globally, with production capacity reaching

200 megawatts with 33 generating units. They were then followed by China, which supplied the most factories with a capacity of 36 kilowatts per ton of cement. This step saved 25-30% of the energy used in the cement industry. Then came the Southeast Asian countries, whose production capacity is less than 200 tons per day, as they contributed to controlling pollution and raising energy efficiency [13].

1.4. ENERGY MANAGEMENT METHODS BEING PROMOTED

It is imperative to conserve energy in manufacturing processes that go through stages to produce a high-quality product and improve operating efficiency, which is the basis of manufacturing processes, starting with the choice of primary materials and the ratio of the homogeneity of these materials. Next comes the role of the equipment used in the production process. Finally, there is the follow up on the procedures for periodic examination of the industrial process and its consequences [14].

1.4.1. Improvements to the Equipment

The energy efficiency improvement in this phase proceeds by applying a minor adjustment of energy conservation in the running production line module. This modification aims to gain extra energy efficiency by supplementing additional or advanced energy conservation modules to the production line or implementing waste heat and gas pressure to gain an extra efficient overall production line solution. An excellent example of energy conservation in the cement plant industry is the effective treatment of the WHR method inside combustion furnaces. In addition to iron and steel works that took place within the generator of the gas pressure, the recovery process, in addition to waste heat recovery, occurs inside the generator of the cement plant [15].

1.4.2. Improvement of the Process

The energy efficiency improvement in this phase returns by applying a significant adjustment in the entire production process where substantial modification is needed to reduce the product line's energy consumption. In addition to higher quality in

products and services, additional savings are achieved in the operating unit in the production line while saving human resources [16].

1.5. AVAILABILITY OF WASTE HEAT

More studies showed how a dismissal of the entire input heat in the dry process plants could reach 40% due to the preheating and cooling processes for the existing gases, as shown in Figure 1.5. It has been observed that in the temperature range between 200-300°C, the amount of heat lost due to existing gases reached 180 to 250 kCal/kg of clinker [17]. The utilization of waste heat becomes a crucial factor for engineers in most plant industry product lines. It has been realized for drying raw material and coal that subsequent waste heat is available, comprising the needs for the drying energy, which can be used as additional energy for electrical power generation as an example [9].



Figure 1.5. Waste heat sub-process availability on a regular basis [18].

1.5.1. Waste Heat Recovery and Power Generation

The preheater and cooler exhaust gas have a noticeable amount of heating value with the use of waste heat being considered worldwide. For example, in Japanese cement plants, it was reported that 41.8% of the total electricity consumption of 19 cement plants considered waste heat as an independent private power plant. Figure 1.6 illustrates the flow diagram of such kinds of architectural plants [19].

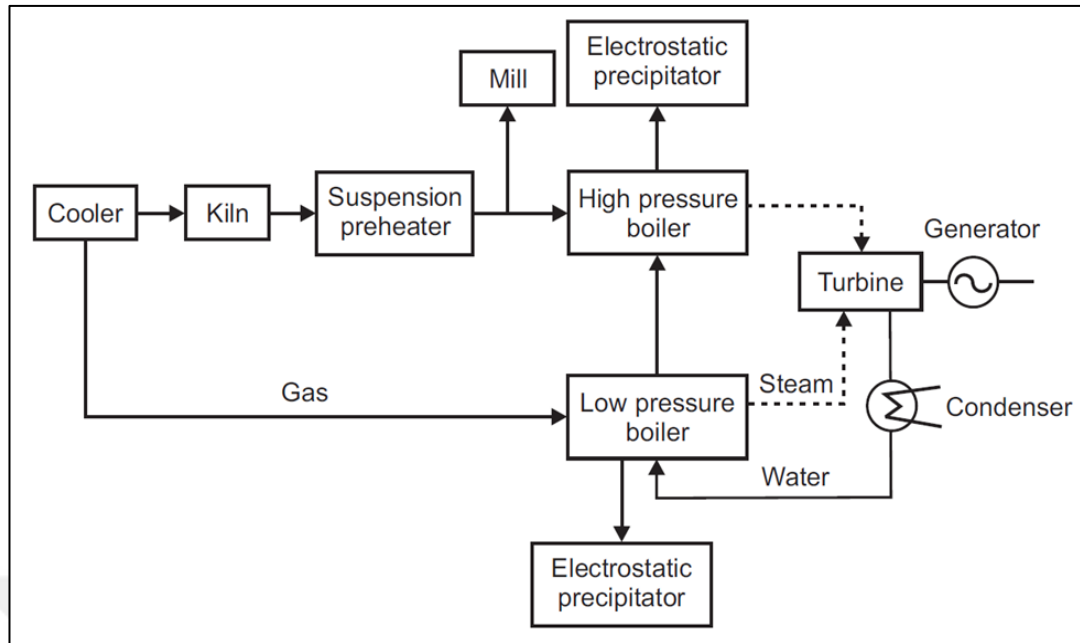


Figure 1.6. Power generation from waste heat recovery [19].

1.5.2. Advantages of WHR in Cement Plants

It has been considered that the implementation of WHR systems, known as power plants, have a considerable improvement measurement concerning energy and production aspects in the cement plant. The occurrence of improvements from the energy and economic aspects can be demonstrated as below:

1. Waste heat conversion into electricity will increase the energy efficiency of the system module of the plants and reduce the discharging of waste heat accordingly.
2. Electricity produced through the Waste Heat Recovery Project in the cement industry helps reduce the demand for electricity from the public electricity grid [20].
3. Captive electricity production leads to a decrease in the corresponding amount of CO₂ emissions.
4. The use of electricity produced within the cement plant reduces the loss of electricity transmission from the public grid and increases its stability.

5. The savings resulting from size reduction reduces overall auxiliary energy consumption, which supplies supplementary gains in electrical additional energy consumption similar to fans, pumps, etc. [19].
6. Water control at the entry stage of the raw mill enables the plant system model to reduce water evaporation by decreasing the water in the cooling tower, in turn leading to a noticeable improvement in the operational model parameters of the running plant. In other words, more power efficiency can be achieved by reducing the raw mill temperature, thus reducing waste gas temperature. As a consequence, extra heat can be obtained and utilized in the plant.
7. Dust agglutination inside the used textile filters can be significantly reduced by utilizing a more modest amount of steam in the waste gas.
8. The potential conservation of drinking water resources can be achieved using a water-saving control mechanism in the cement production plant [21].

1.5.3. Cogeneration Possibilities

Bottoming cycles seem to be an attractive solution for some Indian cement plants by adopting cogeneration technologies where potentially 25-30% require power measured from a plant capacity of 1 million tons. It has been considered that practicing the combination of cycle cogeneration to utilize a coal-based thermal in power plant coupled with grid power cut/failure is substantial mitigation, which is frequently desired in power plants, as shown in Figure 1.7. Practical experience showed the possibility of generating a considerable amount of power, approximately 4.5 megawatts, by using the conventional boiler of waste heat operating under an environment of a 300 TPD plant running on existing gas temperatures between 350°C and 400°C combined with a steam turbine. Studies revealed that the supplementary firing NCB could enhance the power cogeneration by a remarkable amount reaching ranges that extend between 3.0 and 5.5 MW in approximately 20 industrial cement plants. This increase has some dependencies distributed among different circumstances, including the availability of gases compared to the number of PH stages, gases temperature, the drying process of raw material, and coal used by the gases [22].

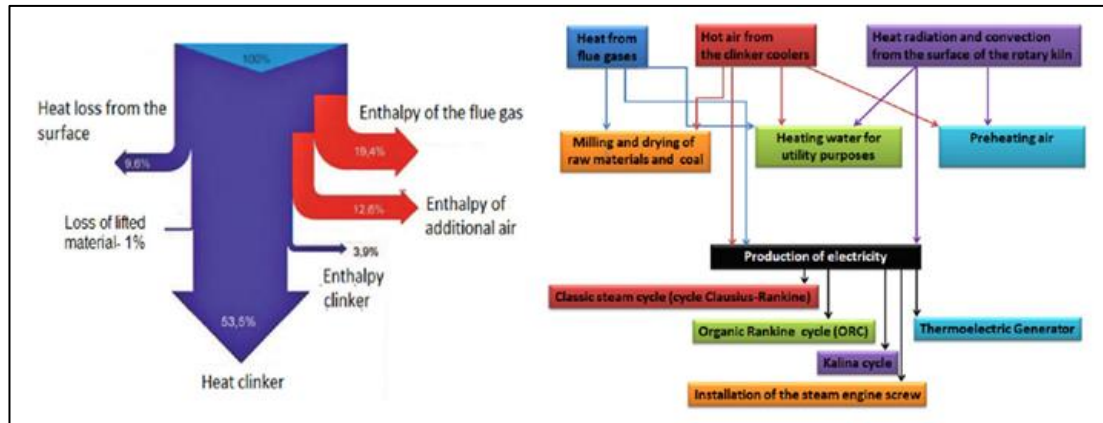


Figure 1.7. Cement kiln heat balance and heat utilization potential [23].

1.5.4. TYPES OF WASTE HEAT RECOVERY APPLICATIONS

There are three systems for generating steam from waste heat in the cement industry, mainly based on the Rankine cycle. These systems consist of:

1. The turbine function that converts thermal energy in steam into mechanical energy to generate energy with an electric generator;
2. Electrical generators generating electrical energy;
3. Condensate to expel the heat of the steam and convert it into its liquid form; and
4. A pump raising the working fluid pressure used from the condenser in the liquid state.

1.5.4.1. Standard Rankine Cycle

The Rankine cycle is defined as the cycle whose function is to convert heat energy into action. Heat is fed from an external source in a closed loop, which usually uses water. This cycle generates approximately 80% of electrical energy worldwide, including solar thermal installations, bioenergy, fossil fuel energy, and nuclear power. Its name goes back to the Scottish engineer William Rankine. The Rankine cycle is the basic building block in the thermodynamics of a steam engine. Water is heated with the hot gases generated from the cement plant, and by using the waste heat boilers, it is transformed into steam, as shown in Figure 1.8. Then its temperature rises above the

saturation temperature and passes to the steam turbine in the form of superheated steam, which expands to generate energy.

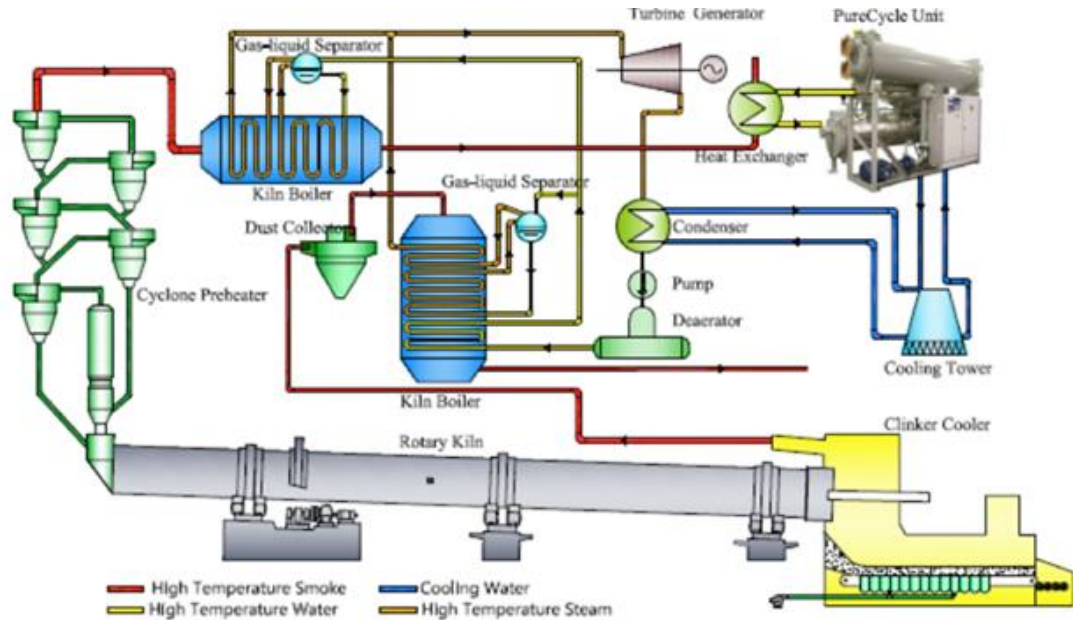


Figure 1.8. Standard Rankine cycle in a cement plant [24].

1.5.4.2. Rankine Organic Cycle

The working fluid for this system is an organic liquid. Heat transfer occurs in two stages, as shown in Figure 1.9. The first stage transfers the heat of the hot gases in the reheating tower and the hot air in the grid air cooler to the heat transfer fluid (water or thermal oil). In the second stage, heat is transferred from the water or thermal oil to the organic liquid. It is better to use water instead of thermal oil for reasons including the amount of electricity spent on pumping oil, 30% more than that which is spent on pumping water. Likewise, the diameter of the pipes containing the oil is greater than the diameter of the water pipes due to the high viscosity of the oil to obtain the same pumping value, leading to an increase in the project cost. In addition, the group of oils that comprise the thermal oil have different properties in nature; with time, boiling components disappear.

Moreover, some thermal oil is broken down if the high temperature of the boiler rises in the short term; therefore, carbon deposits are generated in the fluid and layers that

are difficult to clean, leading to a decrease in the heat transfer efficiency of the boiler. The working source of waste heat in cement power plants is likely to be at somewhat lower temperatures. Therefore, ABB recommends using organic liquids as they evaporate at a lower temperature than that of water. They condense against ambient air at a pressure of more than 1 bar. In addition, organic liquids provide considerable energy when expanding in the turbine. There is no need to create a vacuum in the condenser between the temperature of evaporation and condensation and the pressure ratios. Therefore, it does not need to be as high as possible if water vapor is used as it would be useless in terms of costs or energy [25].

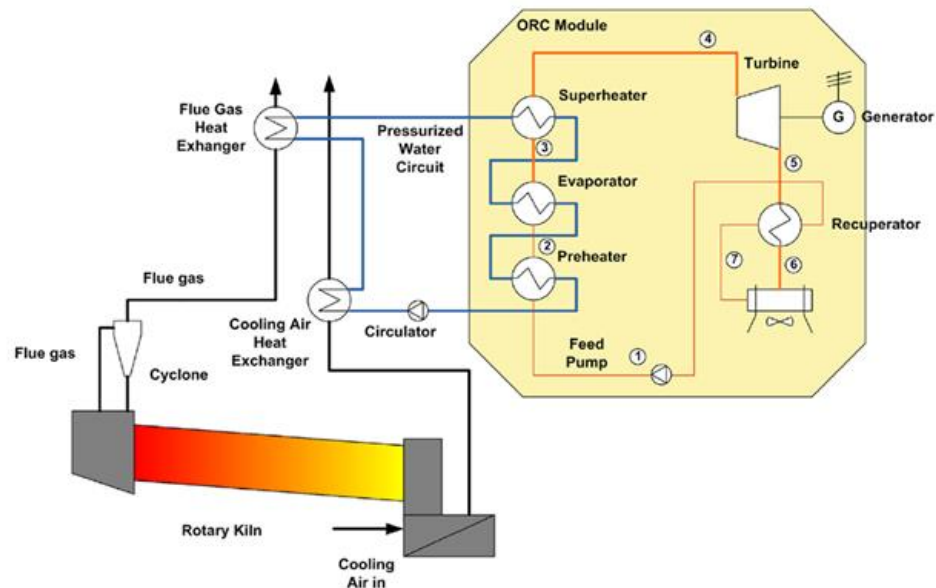


Figure 1.9. Organic Rankine cycle in a cement plant [25].

1.5.4.3. The Kalina Cycle

The name of this system is attributed to its developer Alexander Kalina. This system works in a closed loop, as presented in Figure 1.10, using the working fluid consisting of a mixture of 18% water and 82% ammonia. The equipment of this system is industrial and does not enter the cement production process. The equipment includes boilers to capture the waste heat from a tower reheating and clinker mesh air cooler. This cycle is characterized by working with temperatures ranging from 200°C to 400°C, which means it is possible to obtain the efficiency of this cycle higher than the efficiency of the Rankine cycle by 20% to 40%. This is best in terms of obtaining an

increase in electric power generation. This technology is also characterized by changing the mixture of water and ammonia in different system places, thereby enhancing energy conversion. A separator separates unroasted water droplets from the ammonia to ensure that high-efficiency roasted steam enters a turbine, a condenser to expel the heat of the steam after leaving the turbine, and the pump to compress the mixture towards the boilers. The mechanism of this cycle heats the working fluid (a mixture of water and ammonia). It is then passed in abundance to the evaporator to convert it into saturated steam. After that, it enters the separator to increase the ammonia content in the mixture after withdrawing the non-evaporated water droplets. The liquid enters into a superheater for heating and turns into roasted steam, after which enters the turbine to expand and generate mechanical energy. Via valve No. 10, as shown in Figure 2, the steam leaving the turbine returns mixed with the non-ammonia liquid, which is pressure free. The cooling water expels the heat of the mixture in the condenser. After that, the pump increases the fluid pressure and flows to raise its temperature utilizing low and high temperatures again before entering the provider to close the cycle [26].

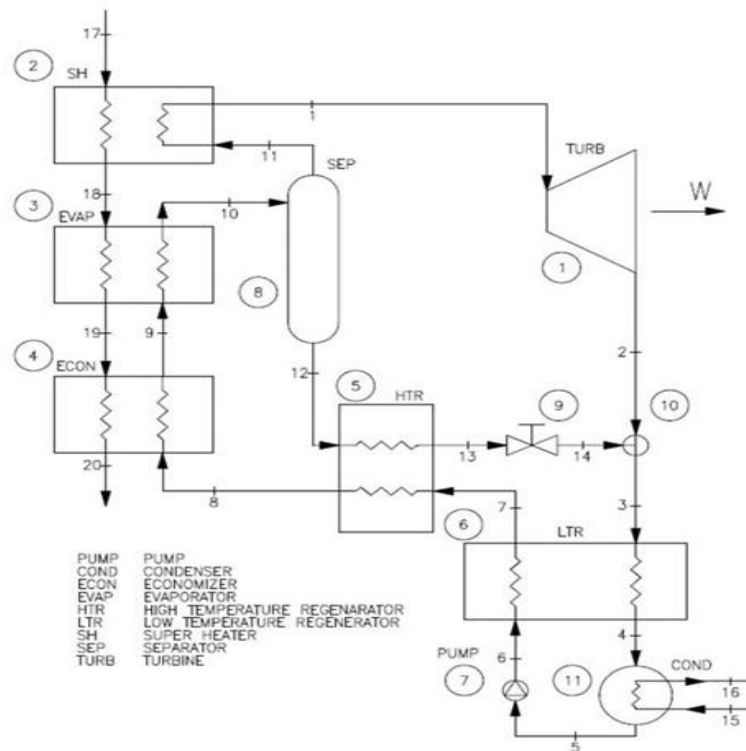


Figure 1.10. Layout of the Kalina cycle in the cement plant [26].

1.6. WASTE HEAT BOILER LOCATION

The location of the heat recovery unit plays a significant and vital role in the processing circuit. The reheating tower has the function of drying the raw materials before they enter the rotating furnace using hot exhaust gases. After these gases emerge, they enter the heat recovery boiler (SP). Moreover, an AQC type boiler is installed after the grid coolant of the clinker, as shown in Figure 1.11. These places are selected for boilers so that the heat recovery system does not affect the efficiency of cement production for which the plant was created [27]. Mentioning the design aspect opens the door to various options available such as heat from cooler excess air. The following are some examples:

1. Consolidating the recovery unit of the waste heat in the primary stage before the control device of the cooler pollution.
2. Consolidating the recovery unit in the tuning stage is calculated by design, for example, after the pollution control device and after or before the cooler ID fan; partially pre-circulating the cooler outlet's excess air, which is outputted back to the cooler air fans of the atmosphere.

Extra fuel firing includes an auxiliary furnace to enhance the recovery heat by utilizing hot air combustion. It is essential to evaluate all these various options before finalizing any system model.

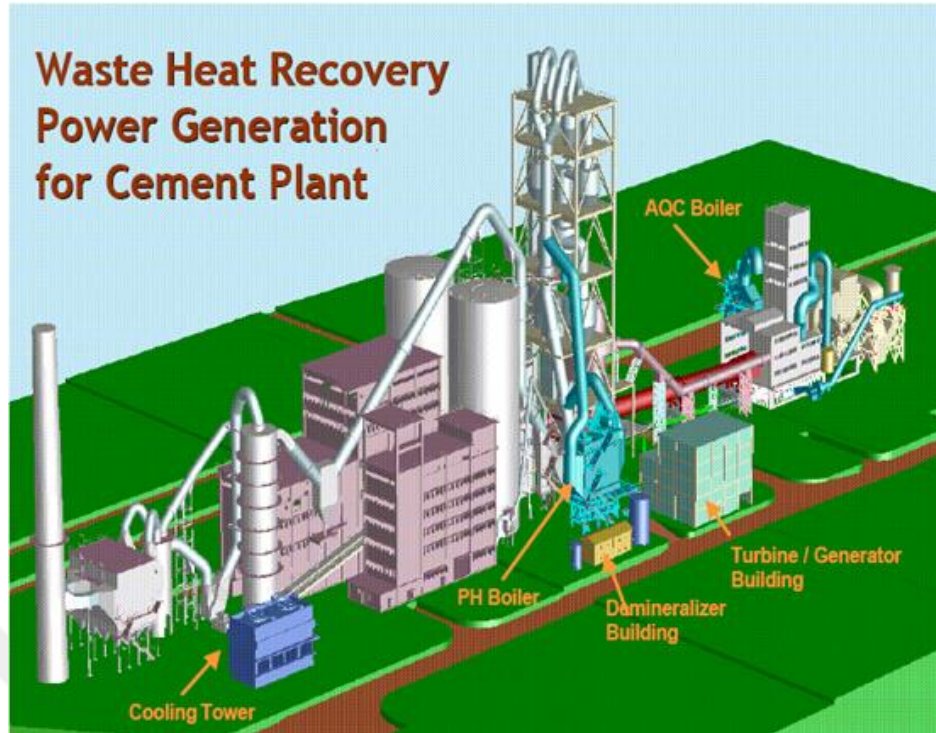


Figure 1.11. Waste heat boilers located in cement plants [28].

It is essential to mention that despite the type, installing the clinker cooler provides quality of the product by quenching the clinker itself. We want to highlight that the clinker functions to overcome the heat preserved when the clinker is red-heated. This function can be achieved by preheating the combustion stage of the secondary air. It has been reported that the heat balance system can retain a considerable amount of calorific heat totaling 13% to 16% of the cooled exhaust gas as consumption during the heat efficiency of the kiln. In addition, there is improvement in the preheater model system where the amount of secondary air required in the combustion process is lower and combined with an increase in the cooler's exhaust gas. Increasing the clinker layer thickness at the grate cooler point is crucial to improve heat exchange efficiency [29].

1.6.1. Appropriateness of the WHR Boiler

A number of researchers have pointed out that waste gases exiting from the exhaust of a preheater and cooler can accommodate very high dust concentrations. It is known that the concentration of PH gases can reach values of 100-120 gm/Nm, which means in return that the values in the exhaust of the grate cooler can reach the order of

60-70 gm/Nm, which reveals the fact that the WHR boiler should deal with and resist the high load of dust. Furthermore, this is one of the essential design perspectives of WHR boilers [30]. The operating model of cement plants is the sustainability and capability to withstand the formation of heavy coating problems due to agglutination of the raw meal dust on the exchange heating surfaces, which in turn causes an extreme capacity reduction and tubes wearing from the fact of particles of the coarse clinker. In summary of all the above, detailed studies are needed to assess the propriety and design of the WHR boiler covering the characteristics of dust involved in the waste gases with concern to dust particle size, the type of stickiness, and abrasiveness [31].

1.6.2. Maximum Temperature of Flue Gas

Flue gases include dust holding alkalis and salts. This aspect has raised a constraint in the maximum scale of waste gas temperature in the production application of the cement plants. A number of studies have pointed out that 600°C is the upper temperature limit of the gas in the steam production model. The alkalis and salts produce sticky and aggressive dust when running at this gas temperature level [32].

1.6.3. Summary

The current running models of the dry process in cement production plants have a dismissal of approximately 40% waste heat of the total heat used as an input to the gas system of the preheater and grate cooler. The thermal efficiency of cement plants can be dramatically enhanced by utilizing the wasted heat as a supplementary power source to generate electricity. Some successful examples of cement plant operating systems in India, China, and some of the southeast Asian countries showed a significant profit in energy conservation and reduced greenhouse gas emissions by employing power cogeneration techniques in addition to alleviating the power shortage problem. The potential of cogeneration technologies in existing operating plans is to reach up to 25-30% of the required power energy of the plants, which already have significant growth in the power efficiency of the system, as shown in Figure 1.12. Nevertheless, some constraints face these plans before they can begin.

● Summary of WHR System

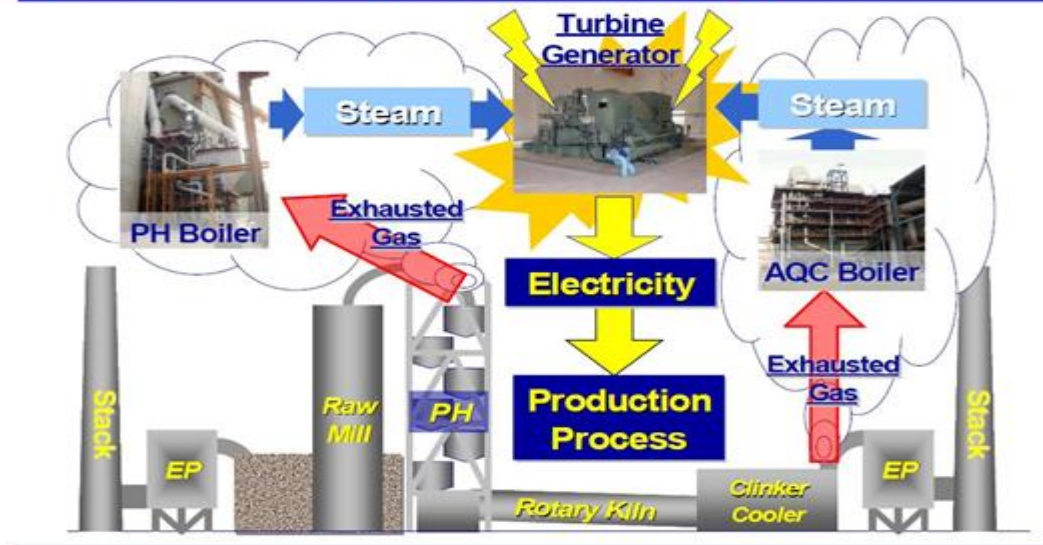


Figure 1.12. WHR framework overview [6].

1.7. RESEARCH GOALS AND MOTIVES

The main objective of this thesis is to recover the waste heat in the cement industry. In contrast, it has many significant benefits on which manufacturers and investors must focus, including:

1. Making the cement factory a producer of electricity in addition to its production of cement, which in turn will reduce the energy consumption spent on the factory and save approximately 30% of the energy consumed in this industry; in other words, there will be an increase in profits;
2. Raising the performance and efficiency of the plant by analyzing the exhaust gases, identifying the operating conditions, adjusting these conditions and thus obtaining a product with high specifications that enhances its position in the market; and
3. Reducing harmful emissions into the environment, especially in factories that have been established near population centers in addition to the capture of waste heat from the atmosphere, which reduces greenhouse gases and global warming, which is an important topic in the present and future.

Dispensing with some traditional cement equipment, such as cooling towers and heavy fuel oil heating exchanges, will help to increase the economic feasibility index. This thesis focuses on the boiler (AQC) in the clinker cooler because the heat in this place is waste without benefiting from it. As for the boiler (PH), its work has been determined on the primary heating of the water. It is used in the production of steam only, while the rest of the heat is left to dry the raw materials before entering the rotary kiln; it is one of the factory design priorities that cannot be changed. Moreover, it affects cement production.

1.8. STUDY OVERVIEW

The WHR system consists of the main part of the boilers to capture heat and to generate steam. The AQC boiler is installed in the Clinker Cooler, and the Boiler (PH) is installed in the Reheating Tower. The second part is a cyclone separator installed before the boilers to capture small particles and dust and prevent them from entering the boilers.

The first chapter of this thesis introduces the cement industry, waste heat and the importance of its recovery. The chapter ends with research goals and motives.

The second chapter of this thesis includes a number of literary studies and the respective authors' views on recovering waste heat in the cement industry and reducing emissions, using this heat to generate electricity, to reduce energy consumption in the cement industry, and to identify research problems.

The third chapter presents the system used for heat recovery and the equipment used with this system. The advantages and disadvantages of some parts used and the reasons for choosing some of them are addressed to produce a system that works in a high-performance manner without technical problems. Taking into account the first examination when installing the system and recording the results; in addition, monitoring the system's performance through periodic inspection ensures the continuity and stability with minor problems of the project's work.

The fourth chapter contains mathematical calculations using thermodynamic equations and EES for the results and drawings of each of the three courses used in this thesis. In addition, we discuss those drawings and results. The chapter ends by selecting the best conditions that will preserve the performance of the plant on the one hand and obtain the net electrical power on the other.

The fifth chapter presents conclusions and recommendations that will shed light on future updates of heat recovery systems in the cement sector to be a springboard for industries with high-energy consumption.



PART 2

LITERATURE REVIEW

This chapter reviews a number of previous studies, some of the literature related to the waste heat recovery project in the cement industry, and the methods used to convert waste heat into resources that can be utilized in this relatively sizeable energy-consuming industry.

Yan et al. [2009] mentioned that the clean development mechanism (CDM) is considered one of several Kyoto Protocol techniques that gained high importance in cement manufacturing operations in China. The researchers discussed how the cement industry's usage rate of waste heat is at a lower level in China than previously, as shown in Figure 2.1. Currently, CDM is used at a high level and contributes to upgrading the cement industry structure. The full use of the Clean Development Technique may help cement companies in China recover any waste created in cement production operations. Conducting Clean Development Technique projects in cement manufacturing process fields focuses on the waste heat of power generation projects that can decrease environmental pollution and provide many social and economic advantages. It supports the development of cement industrial structure and positively contributes to long-term sustainable cement manufacturing upgrades in China [33].

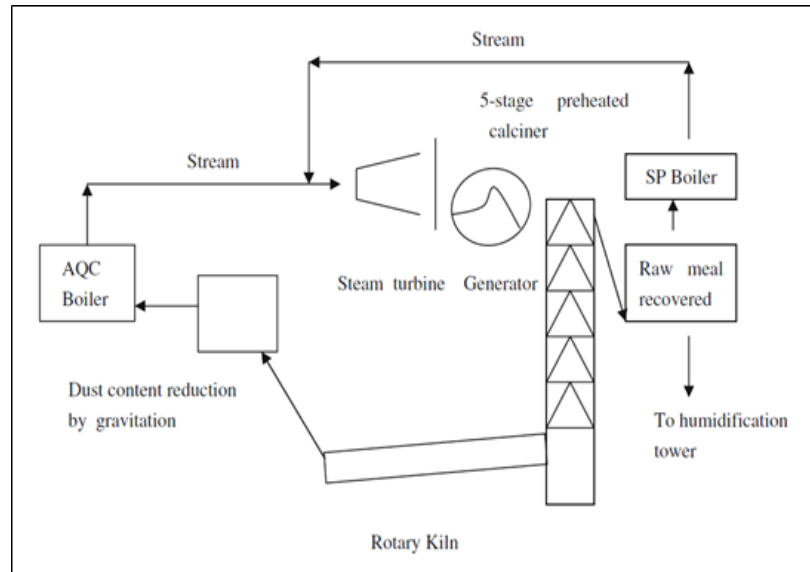


Figure 2.1. Distribution of WHR in rotary kiln [33].

Frank [2009] clarified that the cement industry faces a great challenge in decreasing greenhouse gas emissions because the high amount of emissions reaches 5% of the world's total process emissions resulting from limestone calcination. One of the most favorable technological options is oxygen combustion. The energy penalty for capturing CO₂ is only related to fuel as a reverse on post-combustion capture where sorbent renewal is necessary for the fuel and CO₂ process. In contrast, the more attractive process is the recycling of flue gas and implementing oxygen combustion, which can change the circumstances of the operation. An important study is necessary to create a workable design for the entire conversion of oxygen combustion, as shown in Figure 2.2. Additional costs can be quantified, and the ultimate cost will be balanced between the adjustments and incomes from increased production [34].

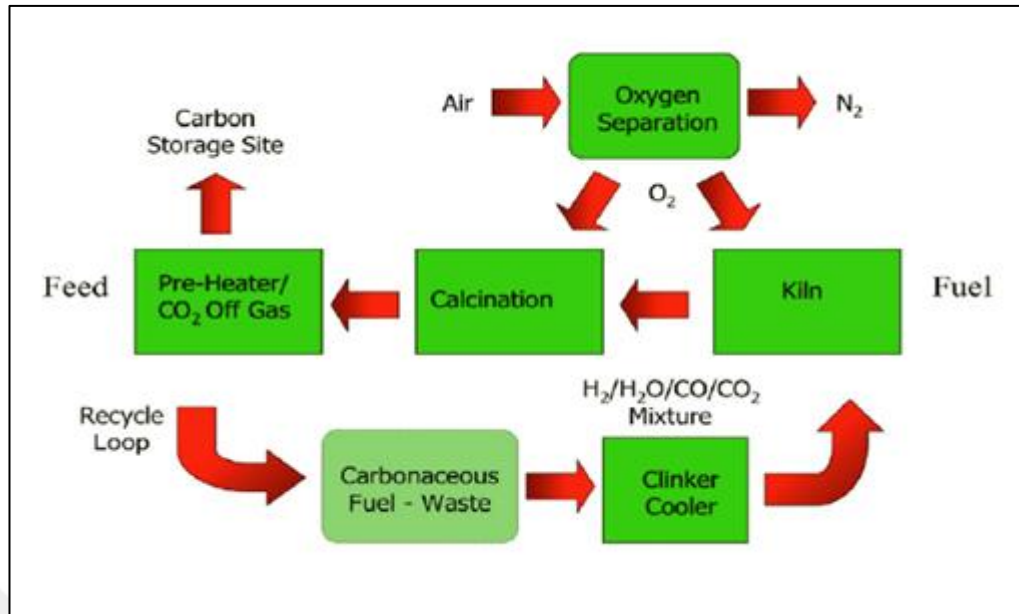


Figure 2.2. Reduced emission oxygen kiln process [34].

Ziya et al. [2010] made observations of heat recovery from rotary kilns at cement plants in Turkey. First, they used operational data of the plant to implement energy analyses, as shown in Figure 2.3. The experimental results referred to the existence of 217.31 GJ of waste heat, representing about 51% of the total heat of the operation. Later, the researchers developed a mathematical model for the new heat recovery exchanger of the plant. They detected that it is possible to use 5% of waste heat with the heat recovery exchanger. The beneficial heat generated could probably satisfy thermal loads for 786 houses in the region with a new heat system area. The proposed system may reduce natural gas and domestic coal consumption by 62.62% and 51.55%, respectively. In addition, when using heat instead of natural gas and coal, CO₂ emissions can be decreased by 1,816.90 kg/h and 5,901.94 kg/h [35].

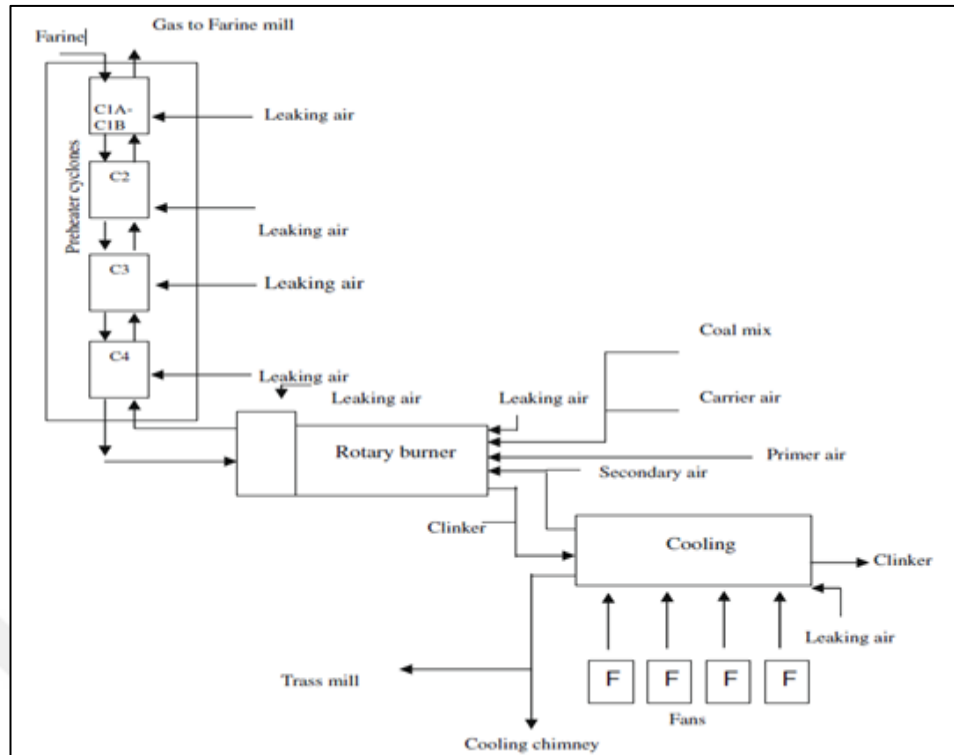


Figure 2.3. Rotary kiln procedure [35].

Mikulčić et al. (2013) mentioned that one of the most carbon emitting manufacturing sectors is the cement manufacturing sector. This industry is the reason behind the emissions of 5% of CO₂ in the world. Thus, it is a suitable sector to organize the emissions of CO₂. By considering the significance of the cement manufacturing process in Croatia, and because the country will soon become a member of the European Union countries, the study analyzed the possibility of decreasing the emissions of CO₂ in a cement manufacturing plant in Croatia. Many measures are used to decrease the emissions of CO₂ in the cement industry, including using waste heat instead of energy, technologies to capture and store CO₂, decreasing the clinker to cement rate, using alternative and biomass fuels, and using alternative raw materials and energy efficient combustion processes. Currently, cement manufacturing uses a rotary kiln composed of calcining and a multi-phase preheater, as shown in Figure 2.4. Other improvement to cement operating conditions are still needed because the use of cement calcines is a comparatively new technique. Moreover, the study highlighted the results of computational fluid dynamic replications used to investigate the combustion emissions process. The previously highlighted measures with mathematical studies can decrease the cement industry's impact on the environment

in Croatia. This may make it more reasonable with cement plants in European Union countries [36].

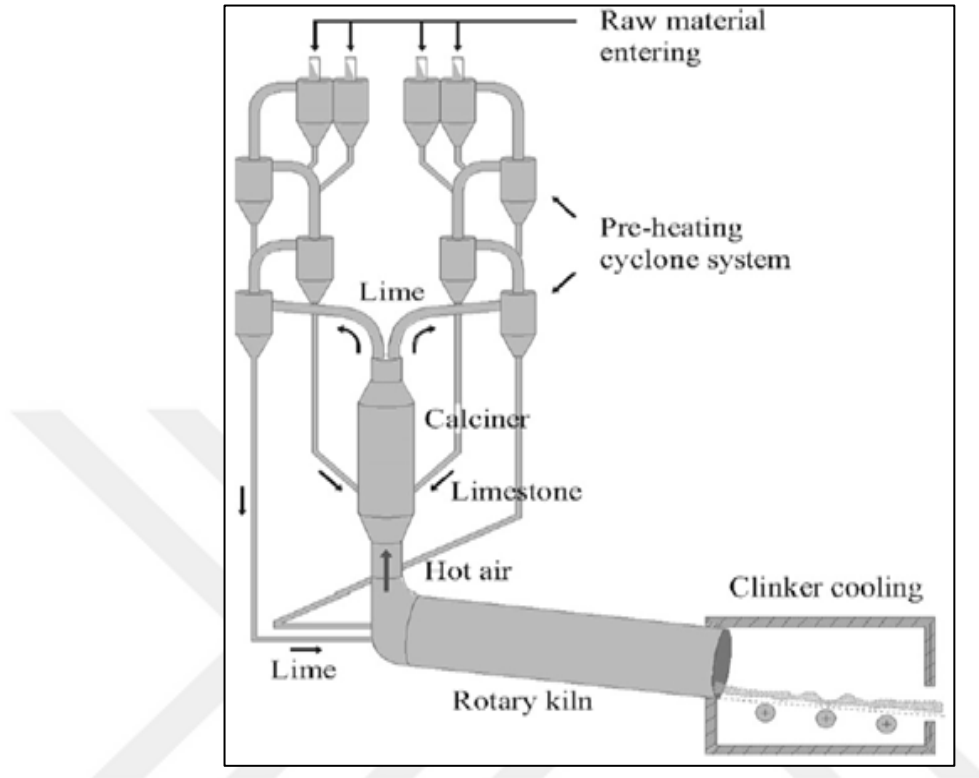


Figure 2.4. General pre-processing in a cement manufacturing plant [36].

Karellas et al. (2013) clarified the procedure used to produce a distinctive cement, as shown in Figure 2.5. The authors mentioned that the energy used is 75% for thermal energy and 25% for electricity. The process is characterized by high heat loss, especially the flue gases and the ambient air stream used to cool the clinker (approximately 35%-40% of the heat loss process). Nearly 26% of the heat input into the system is lost by the clinker discharge, radiation, dust, and convection loss of the kiln and the preheaters. The heat recovery system is used to decrease emissions by increasing the efficiency of the cement plant. The study aimed to investigate and compare two approaches to Waste Heat Recovery (WHR), the first being the Organic Rankine Cycle (ORC), and the other being the water-steam Rankine cycle. The practical study showed that the water-steam technique was better than ORC with exhaust gas temperatures above 310°C. In the end, the authors evaluated the most effective solutions. WHR installations in cement manufacturing may decrease

electrical consumption operating costs and, therefore, be a suitable investment for five years [25].

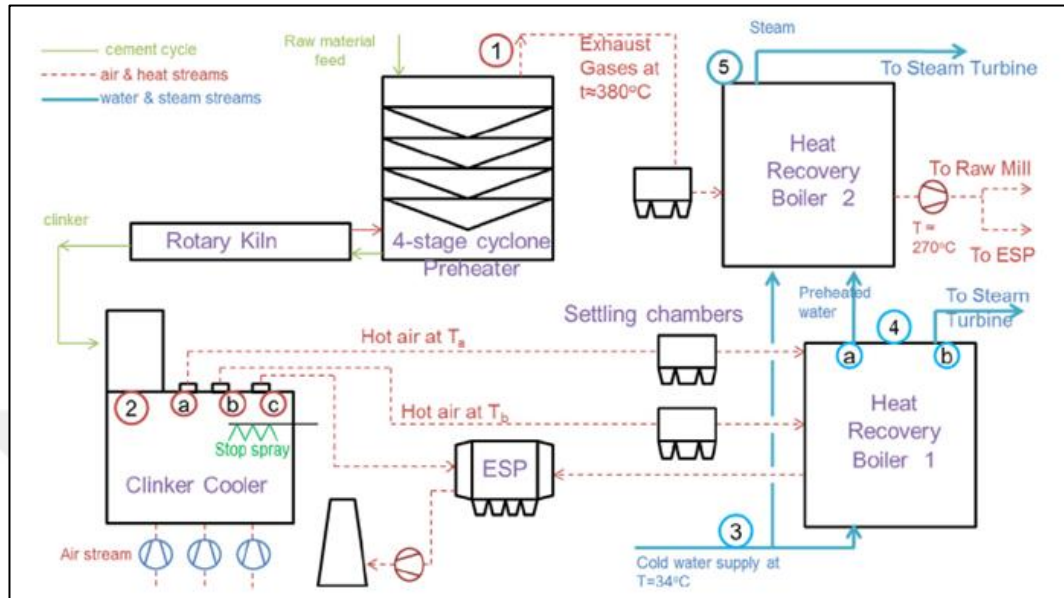


Figure 2.5. WHR system of a typical cement factory [25].

Brunke et al. (2014) stated that cement is considered a majority good correlated with population growth. Since global sales are constantly increasing, the demand for cement in Germany is intense. However, cement production accounted for only 3.8% of the total energy consumption in Germany and 2.9% of total CO₂ emissions in 2012. The researchers evaluated the energy conservation and decrease of CO₂ for 21 notable measures: organic fuel, electricity conservation, and CO₂ decrease cost curves. In the experimental study, the researchers considered the present efficiency of plants and used the boundaries of two systems: a process boundary of benchmarking measures and a capacity boundary to calculate the total probabilities, as presented in Figure 2.6. They measured the economic conservatives and probability of abatement for 2013 with 3.4% fuel and processes related to CO₂ emissions in 2012, 0.7% of electricity, and 4% fuel. The sensitivity results showed that the procedures to preserve electricity in cement grinding might compensate for Germany's electricity tax increase. Instead, the cost of products associated with energy presented high sensitivity against increasing the prices of CO₂. Without major process innovations, including low carbon cement, prices of CO₂ until 2025 accounted on average for more than 40% of total added value

that refers to the European Union ETS directive and the risks of carbon leakage in the cement industry [37].

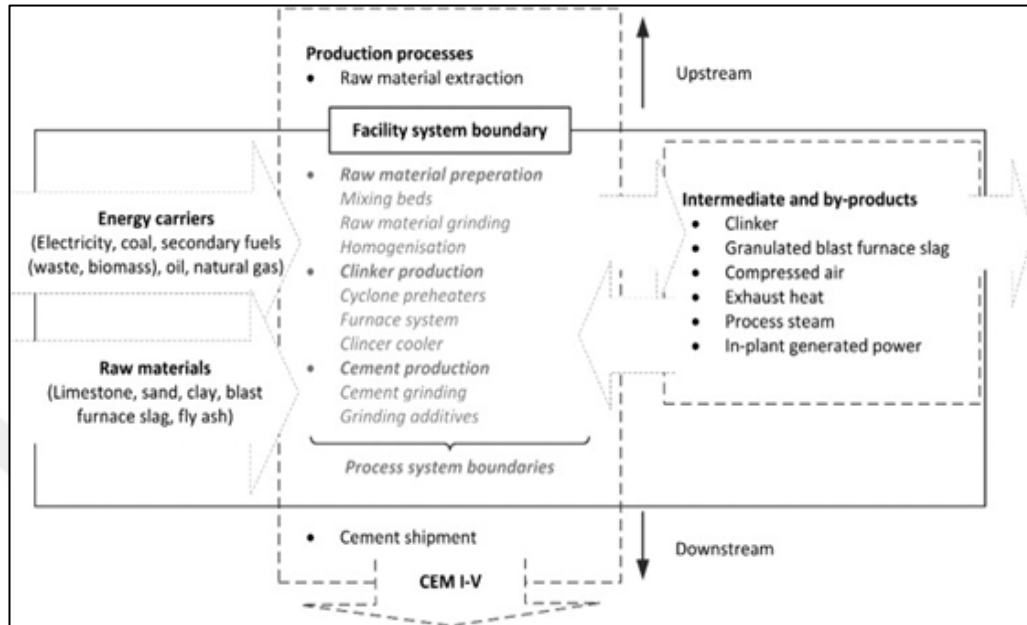


Figure 2.6. Typical scheme of production operations in a cement facility [37].

Luo et al. (2015) stated that the production of Portland cement comprises one of the heaviest industrial productions in terms of energy usage. Manufacturing Portland cement comprises energy consumption of $110\text{-}120 \text{ kWh}\cdot\text{ton}^{-1}$. The cement rotary kiln is considered one of the basic pieces of equipment used in the cement industry, as shown in Figure 2.7. Between 10% and 15% of the energy consumed to produce the cement clinker is directly dissipated into the atmosphere with the external appearance of a rotary kiln. The researchers state that there is an urgent need for innovative technology to preserve energy in the cement industry, and have proposed a new thermoelectric waste heat recovery system to reduce heat loss in cement rotary kilns. The system is arranged as thermoelectric generation units ordered longitudinally in a secondary coaxial with the rotary kiln. They developed a numerical model to estimate WHR performance. The discussions of the study are majorly focused on energy savings and electricity generation by taking a $\Phi 4.8 \times 72 \text{ m}$ cement rotary kiln as an example. The experimental results of the study showed that the $\text{Bi}_2\text{Te}_3\text{-PbTe}$ hybrid thermoelectric waste-heat recovery system may create approximately 211 kW of electrical power and save 3,283 kW of energy. The kiln provided by this system might

recover more than 32.85% of the lost energy as consumed energy through the kiln surface, which is helpful when compared with a kiln without a thermoelectric recovery system [38].

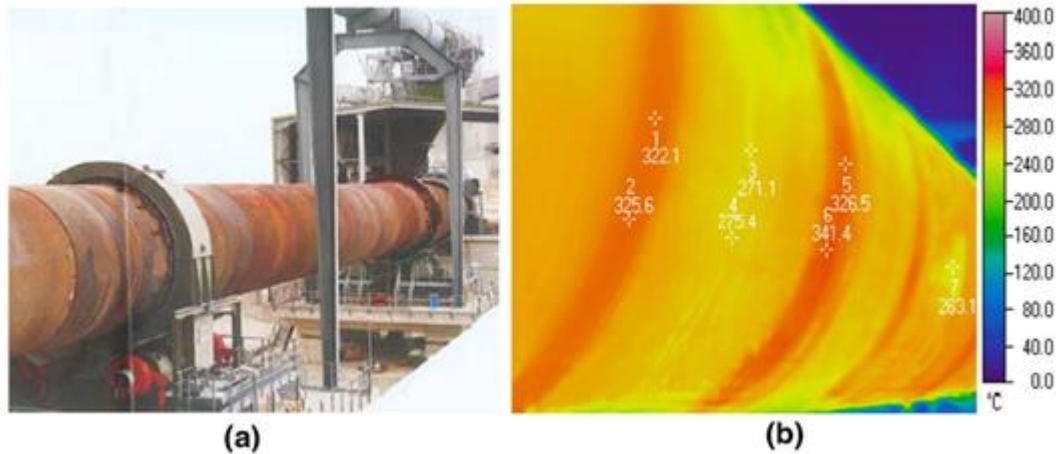


Figure 2.7. (A) Rotary kiln; (b) Temperature distribution of the kiln shell as shown by thermal imaging [38].

Guo et al. [2015] investigated the effects of various working liquids on Organic Rankine Cycle (ORC) performance. Three working liquids were selected, and a mix that matched with a heat source and a mix that matched with a heat sink and pure working fluid were chosen for the research. The researchers constructed a thermodynamic in MATLAB composed with REFPROP through which the physical features of the selected working fluids could be developed. The exhaust flue gas of the boiler was their heat source for the ORC with a 240 MW pulverized coal-fired power plant, as presented in Figure 2.8. Many signs, including the degree of super-heating, inlet expander heat, exergy destruction distribution, mass flow, the influence of recuperating, volumetric flow and thermal efficiency, were studied. The experimental results of the research showed that the mixture that matched the temperature sources was characterized by low temperatures and that the mixture that matched with the heat sink had higher in efficiency. The ratio of heat exchange in the economy to that in the evaporator was higher with evaporation pressure. There were no optimum working fluids for the fundamental indicators (thermal efficiency, mass flow, heat exchanger area, volumetric flow, etc.). A suitable working fluid had to be selected by considering the cost of investment and the benefits of power generation. Moreover, the cost-benefit rate of the suggested ORC was evaluated [39].

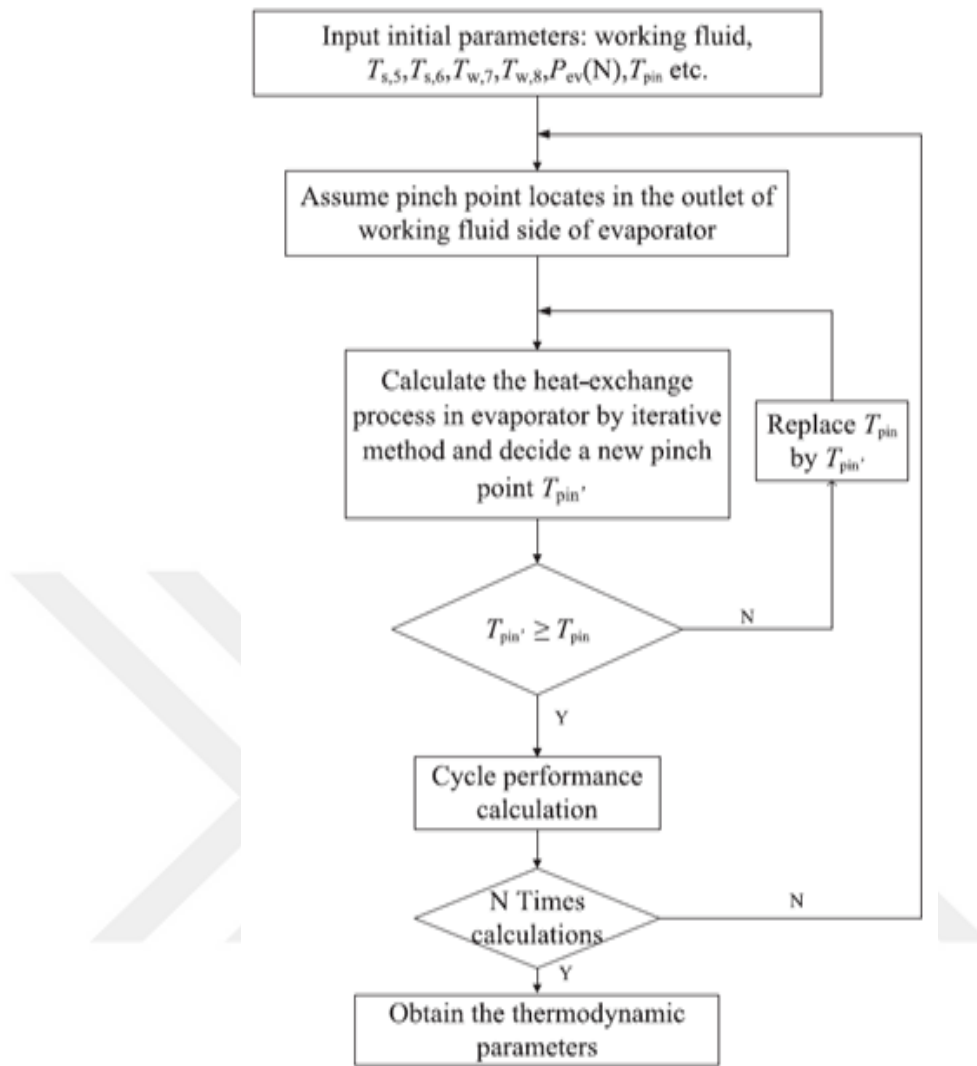


Figure 2.8. Diagram of the simulation process [39].

Amini et al. (2015) suggested a transcritical CO₂ Rankine cycle to recover low-grade waste heat at the Yazd combined-cycle power plant in Iran, as shown in Figure 2.9. This plant includes many power generation modules, comprising one 132 MW steam turbine and two 159 MW Siemens SGT-5-2000E gas turbines. The plant can generate extreme power when exhaust temperatures decrease from 150°C to 70°C. Approximately 6.3 MW is conserved for the selected power plant with a nominal 450 MW of power generation at the previously declared operational point [40].

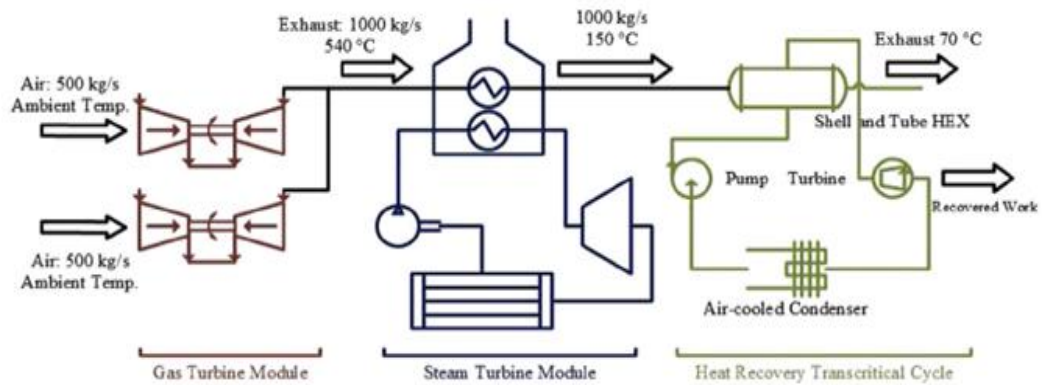


Figure 2.9. Diagram of Yazd combined-cycle generating station [40].

Maalouf et al. (2016) mentioned that low-temperature flue gases (less than 120°C) generated by industrial operations could be recovered to generate electricity and develop an effective means to decrease the primary consumption energy and emissions of CO₂. The high temperatures in wet flue gases can be recovered if the water vapor in these gases is reduced. The technical selections included condensation of indirect water vapor. Heat was conveyed between the two fluids (the working fluid and flue gases) using an intervening wall (usually a fin-and-tube heat exchanger). Direct contact water vapor condensation recovery would directly mix flue gas and cooling fluid (water) through the condensing unit. The study investigated the two-recovery process using ORC, as shown in Figures 2.10 and 2.11. The most effective heat recovery diagram is indirect contact condensation in terms of net output power. The direct contact heat exchanger gained great interest because of the no heat-transfer surfaces being exposed to corrosion. During indirect water vapor condensation contact, the inlet flue-gas wet-bulb heat regulates the operating temperature levels throughout the system. It limits the temperature and water flow. The maximum net turbine power of the direct contact system is to reach final water heat near the heat of the flue gases [41].

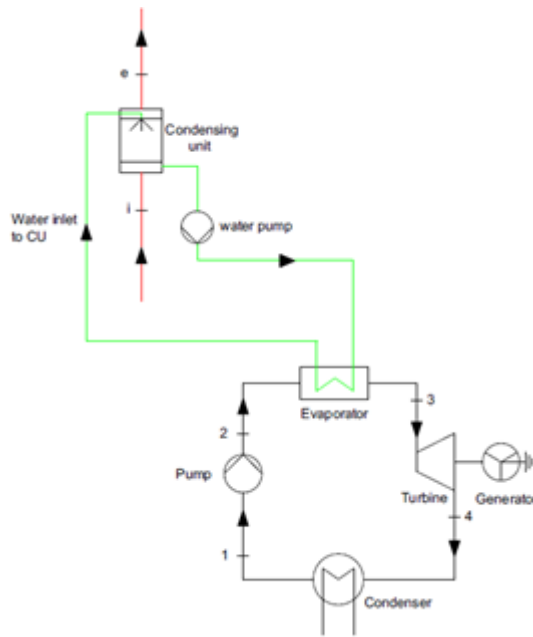


Figure 2.10. ORC with condensate in direct contact [41].

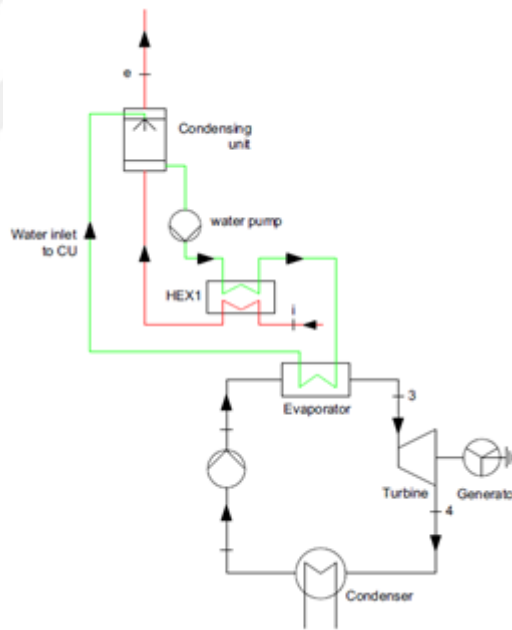


Figure 2.11. A phase of hybrid heat recovery [41].

Huang et al. [2016] mentioned that the cement industry in Taiwan comes in the second most energy-intensive sector. A bottom-up model-based evaluation is used to analyze the scenario of energy-saving opportunities until 2025, as shown in Figure 2.12. Experts in Taiwan have supported the analysis of the study in detail through interviews. The simulation results detected that by 2035, 18 energy-effective

techniques might result in a 25% saving of electricity and 9% savings of fuels for fuels through the technical diffusion scenarios. This possibility amounts to approximately 5000 TJ/year, of which 91% can be conducted efficiently, assuming a decrease ratio of 10%. Decision-makers in the country should support the quick diffusion of these technologies. The supporting operation can be undertaken by many methods such as reducing the share of the clinker, which is currently controlled by at least 95% and extends the ban on creating new cement plants by replacing the current capacity with new and inventive plants in the following years. In addition, support can be given by using substitute fuel that presently still occupies a good position in Taiwan [42].

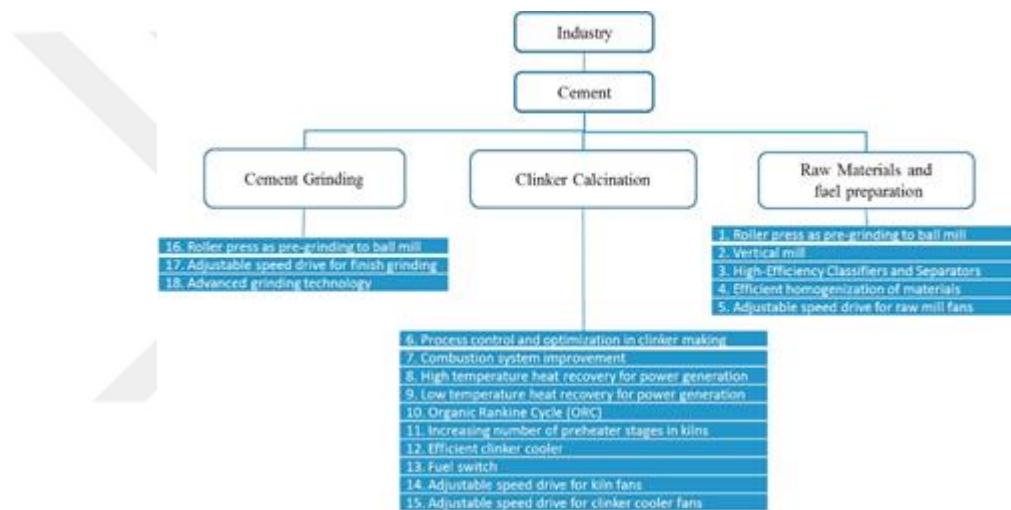


Figure 2.12. Three-level hierarchical structure of the bottom-up model [42].

Boldyryev (2018) mentioned that since the most used material in modern infrastructure and housing is cement, the study analyzes the energy efficiency of the cement manufacturing process for specific cement plants, as shown in Figure 2.13. The cement industry is considered to be one of the foremost energy consumers, including carbon, one environmental pollution element that comprises approximately 5% of total global pollution. The consumption of energy is the largest part of cement industry costs and it has a great impact on the prices of products. Since it is clarified that the infrastructure projects in modern society lead to a high level of sustainability and economy of states, decreasing the production costs of cement is a critical issue. The researchers analyzed the energy consumption for specific Croatian cement plants to identify the lowest energy goals and suggested paths to improve energy efficiency. The process integration method was used in the study. However, the cement plant's

characteristic necessitated updating the methodological steps of the research to suggest actual paths for the retrofit project to achieve the optimal least temperature between the process streams. Many streams, such as air streams, gas, and solid particles, must be cooled down quickly. These facts become very complex because of the special construction of the process equipment that may cause the probability of heat transfer among some streams. The major goal of the study was to determine the possibilities of actual energy savings and suggest a solution to the new concept of HEN, which avoids process traps and delivers a reasonable retrofit. When HEN was constructed, the highest heat recovery for producing a specific type of cement was identified and improved. The researchers concluded that it was possible to decrease the energy consumption for cement plants by 30%, with a probable recovery period of 3.4 months. The implementation of this retrofit project helped to increase the plant's profitability and improve the cement industry process [43].

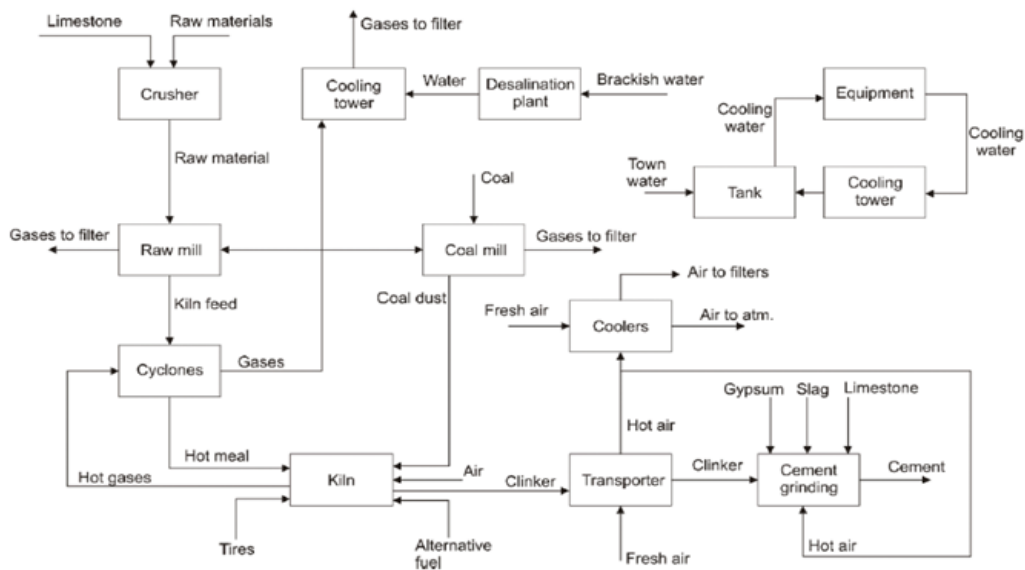


Figure 2.13. Primary flow sheet of the cement manufacturing process [43].

Ahmed et al. (2018) showed that the organic Rankine cycle (ORC) transfers the traditional energy system to the steam cycle. It would use organic working fluids including hydrocarbons and refrigerants, rather than water. The renowned research interest of ORC emphasizes its tolerant adoption as a pioneering technology to convert low and medium temperatures, i.e., $80^{\circ}\text{C} < T < 300^{\circ}\text{C}$ heat resources, to power. Figure 2.14 shows the flow diagram of the ORC. The actual data comes from the

selected local cement plant that determined the state of the design with the working fluid influencing the cycle efficiency. The selection of fluid is considered a basic issue for good cycle performance because the physical properties of the optimal thermos are based on the heat source. The study clarified the organic Rankine cycle results mutually with the gas turbine to transform the waste heat of the gas turbine to electric power and selected R134a working fluid for the design of the study. Approximately 1 MW of power could be created using ORC. An exergy analysis was performed using actual data, which clarified that most of the energy would be lost in the working turbine [44].

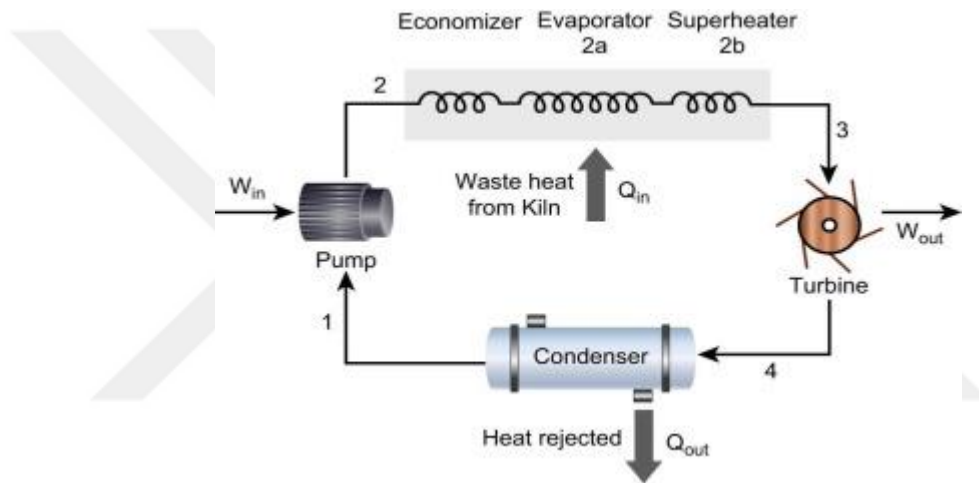


Figure 2.14. ORC flow diagram [44].

Dan et al. (2019) studied the production of cement related to the probable effects of environmental emissions from the perspective of conversion efficiency. The aims of the study were to analyze the thermal process comprising resources and energy accounting and conversion with exergy metrics. The recycling, loss, and exergy conversion efficiency of resources were computed by considering each part of the cement industry chain. The results of the study showed that the milling phase had the greatest conversion efficiency following clinker calcination. In contrast, those associated with raw material preparation and the preparation of crushed coal were very low. Because of the temperature difference, the clinker calcination part had a high exergy loss rate following the waste gas section, as shown in Figure 2.15. The preparation part of raw materials included low exergy loss without a high-temperature phase. The cement milling section and pulverized coal preparation were characterized

by the lowest losses of energy. In addition, the coal power preparation part would include the highest recycle rate, followed by the raw material preparation with high amounts of sensible exergy. In contrast, the clinker calcination part contained a low rate of coal combustion [45].

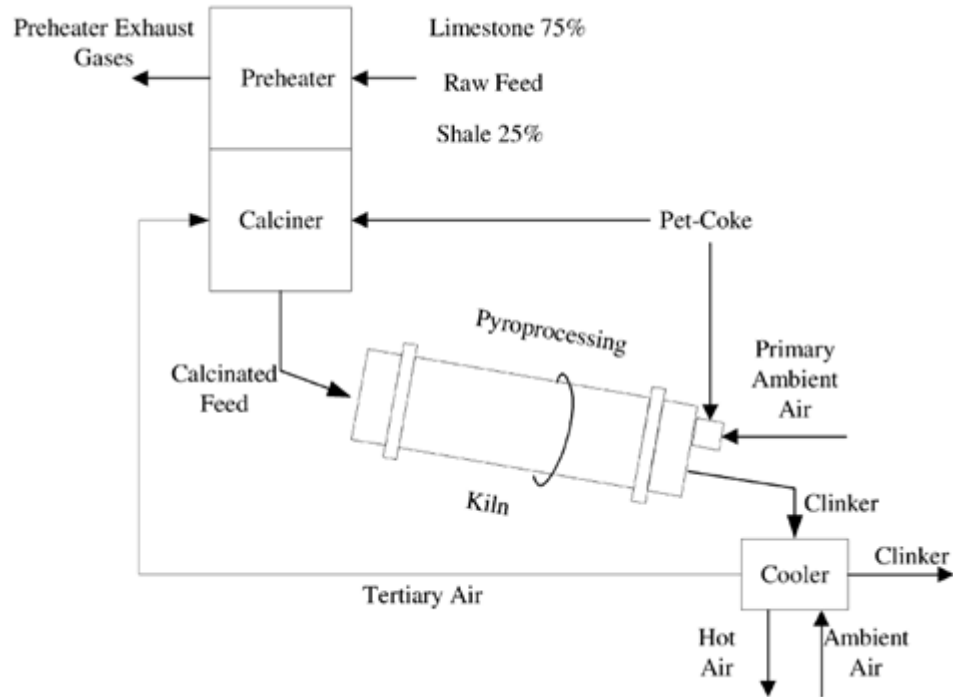


Figure 2.15. Manufacturing clinker [45].

Naeimi et al. (2019) mentioned that one of the highest heat recovery potentials globally is the cement industry. They investigated the technical design practicability of WHR from gas engines to generate electrical power for Unit-8. The study was implemented at the Tehran Cement plant, as shown in Figure 2.16, and included a proposition and comparison of two different methods of energy recovery. The first scenario included using only a heat recovery boiler with aggregate mixed gas entering the boiler before arriving at the grid cooler and preheater. The other scenario included a vapor mix that would arrive in the turbine of steam. The study aimed to analyze, design the gas engine, and use FORTRAN software to calculate the practical part. It must be mentioned that air conditioning in the place of management consisted of calculating the heat load of a gas engine. The third analytical section, the codes, is a computation process of the joint heat recovery system with the gas engine. The study findings showed that the quantity of the recovered temperature in the first and second

scenarios was 23,931 kJ/s and 21,253 kJ/s, respectively. The power generation cycle proficiencies in the first and second scenarios were 23.5% and 22.2%, respectively [46].

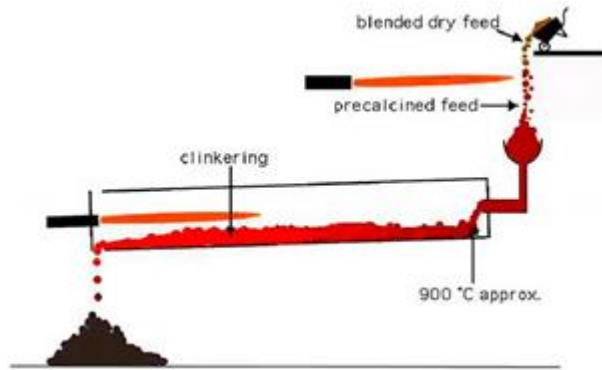


Figure 2.16. Method of using a dry kiln.

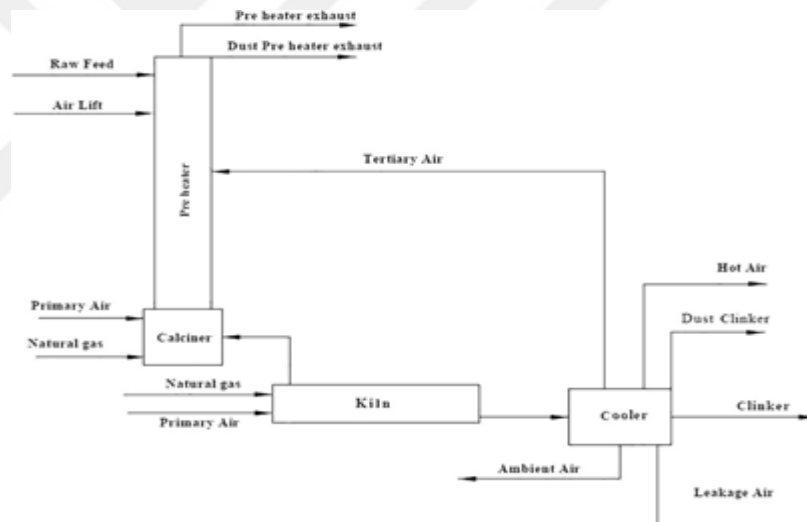


Figure 2.17. Diagram of the system analyzed by Naeimi et al. (2019) [46].

Moreira et al. (2019) studied the economic performance and thermodynamics of simple and regenerative ORCs under variable circumstances, as shown in Figure 2.18, the first time in high temperature and the second time in low temperature. The researchers used WHR in cement plants in Brazil with productive clinker sizes ranging in size from 3,000 tons/d to 6,300 ton/d. After selecting the most appropriate organic fluids, the cycles were modeled in terms of economic features and thermodynamics using the Engineering Equation Solver (EES) software. The critical operating parameters of the processes were improved using the same software taking the genetic

algorithm approach. The study findings showed that organic fluids with high performance from exergy efficiencies, thermal, and net power output were R123 R1 and R141b, respectively. In terms of all the cycles analyzed, the period of payback would be less than two years. The net existing value varied between 130 to 170 million reales, and the interior return ratio surpassed 80%/year. The suggested ORCs could generate between 4,000 kW and 9,000 kW or approximately 80 MW in the cement sector of the Brazilian state of Minas Gerais. This therefore would eliminate the production of 221,069 kg of CO₂/year. It should access particular investment and electricity generation costs that vary between 2,250-4,300 R\$/kW and 0.09-0.11 R\$/kWh, respectively. Depending on the findings of the study, it was concluded that the suggested ORCs for the WHR of cement manufacturing in Brazil would be ecologically stimulating and exceptionally reasonable in terms of the technical and financial features [47].

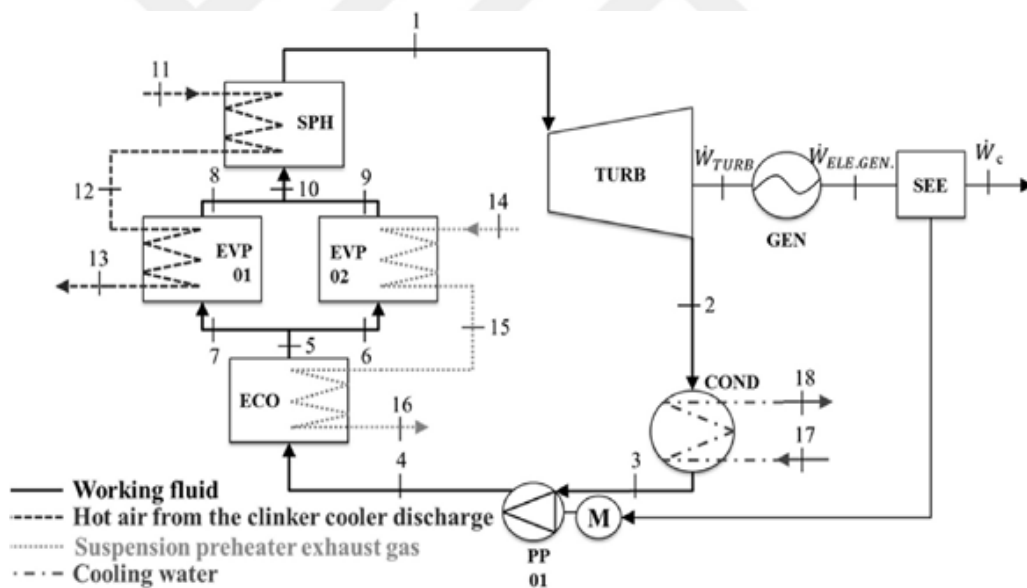


Figure 2.18. WHR in a cement plant by basic ORC [47].

Mirhosseini et al. (2019) mentioned that a rotary kiln could be considered a primary tool in the cement manufacturing process on a large scale. The heat of the shell may provide access to hundreds of degrees Celsius. The researchers designed an arc shape absorber with temperature delivery across the absorber edge being obtained mathematically, as shown in Figure 2.19. The hot side of TEGs were the computed temperature that would recover the thermal absorber energy. Access to the greatest

energy production was the scale of the design of the thermoelectric system. The length of the absorber was separated into various divisions to access the local parametric design power. To obtain an effective TEG design in each part, the impact of the major parameters, including the length of leg, fill element of the TEG, and heat resistance of the heat sink, were investigated [48].

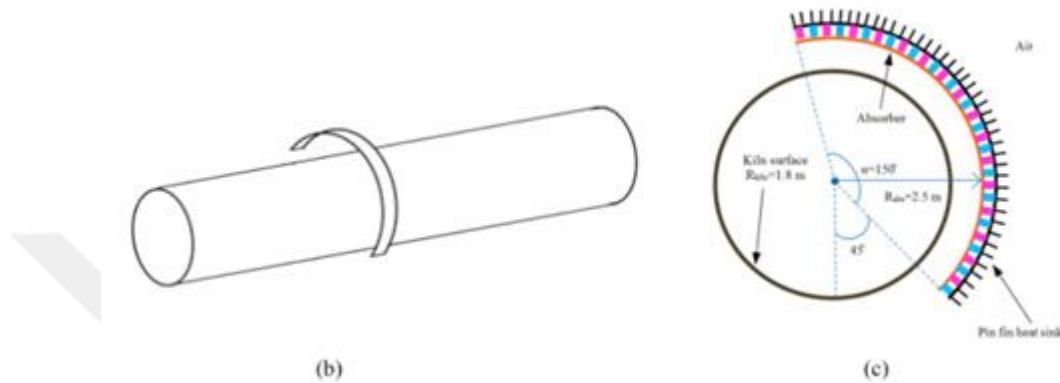


Figure 2.19. Heat absorption diagram around the kiln [48].

Temperature, rapid air, and aquarium temperature affect the performance of absorbers' finned temperature. Magnesium tin silicide (Mg_2SiSn) and B-phase zinc antimonide (Zn_4Sb_3) were selected as the p- and n-leg thermoelectric materials of the TEGs, as shown in Figure 2.20. Correspondingly, due to the comparatively higher performance above the measured scope of adequate heat, the study findings showed that good planning of the pin-fins is more efficient for the high performance of system and power generation compared with the in-line fin arrangement [48]. Furthermore, the assessment of the results showed that the highest coordinated power output in every part against the fill element and leg length could identify the research. Moreover, it is shown that low-fill elements between 0.05 and 0.2 can deliver comparatively the same highest power as high-fill elements.

The economic assessment was performed to detect the ideal design of the TEG device for low investment cost and high power generation. The study took into account many parameters of the cost function, including manufacturing costs related to processing the bulk material (CM, B), real manufacturing costs (CM, A), heat exchanger costs (CH-EX), costs of bulk raw materials (CB), installation costs (CI) and the balance of

system costs (CBoS). The study results clarified that the dominant parameter of system cost is a heat sink [48].

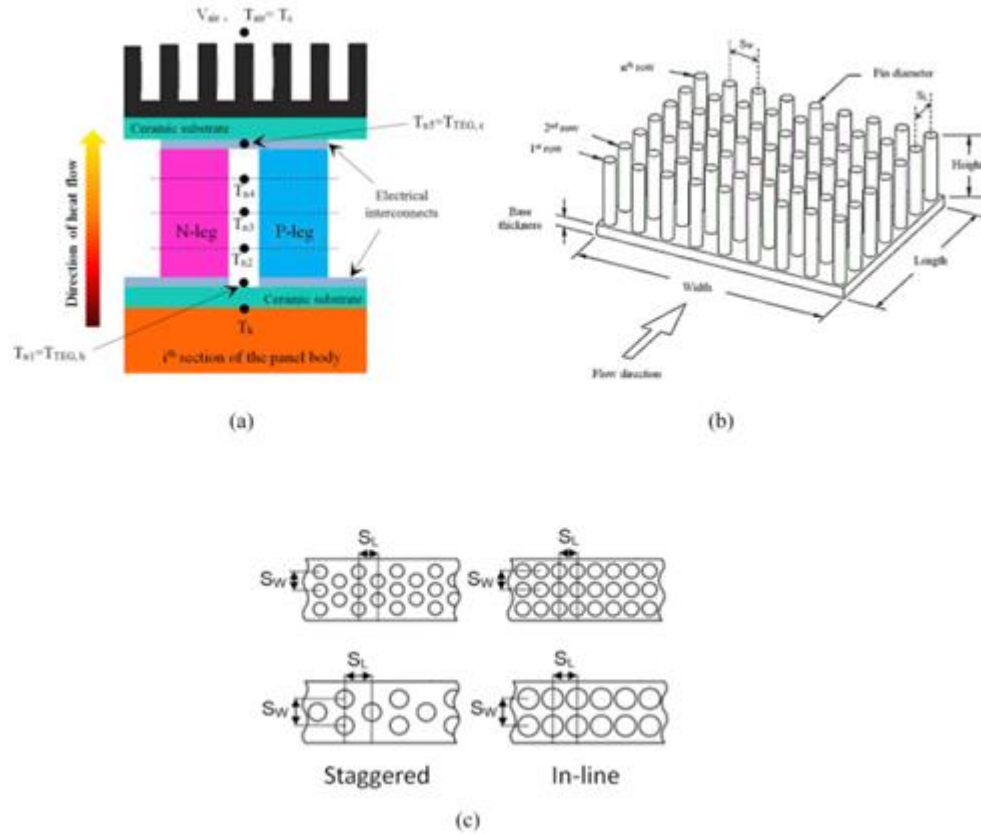


Figure 2.20. Heat absorber components around the kiln [48].

Júnior et al. (2019) investigated the Kalina cycle assessment, which exists to approximate the possibility of generating electricity from exhaust gases of the cyclone preheater for the rotary kiln in Brazil's cement plant the production capacity of the clinker is about 2.1 thousand tons. The cost approximation, thermodynamic, heat transfer, and enhancement models have been developed in the EES to approximate the cycle pieces dimension of the equipment. In addition, assessing the Kalina cycle performance performs its enhancement associated with net power, thermal and energy efficiency, as well as the particular cost of electricity generation. It was observed that the concentration of ammonia in the evaporator's outlet decreases the pinch point in the evaporator, thereby increasing the net power. In contrast, an increase in the turbine inlet pressure decreases the cost of generated electricity. The condenser and heat recovery boiler is significant for approximating the investment cost for cement

manufacturing waste heat recovery cogeneration plants, as shown in Figure 2.21. With relatively high costs in electricity generation, maximizing power generation is the suitable goal function to enhance the studied Kalina cycle. Power generation values, thermal efficiency (0.233), and energy (0.478) 2,429.056 kW are similarly favorable. In the tariffs of the Brazilian market, the cost value acquired (~ 0.2847 R\$/kWh and 5,507 R\$/kW) is reasonable in the electricity sector scenario of Brazil in the next decade of the 21st century [49].

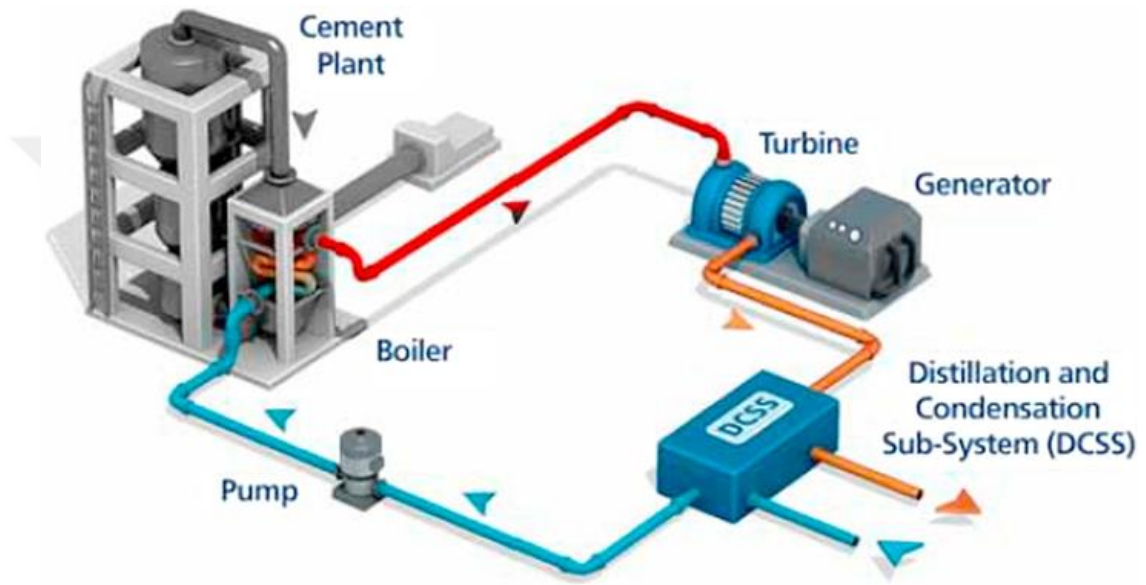


Figure 2.21. In the cement industry, WHR is idealized for electricity generation using the Kalina cycle [49].

2.1. RESEARCH PROBLEMS

The hot air generated by cooling clinker and exhaust gases is the main heat carrier from the source. The main challenge to the WHR process is that this conveyor must be free of dust and small particles. The clay is from the raw materials used in the cement industry (the clay being an adhesive material). Therefore, it can adhere to the surface of pipes. Moreover, it may cause corrosion in the pipes because of friction as the dust contains a small amount of clinker material, characterizing its hardness. All these problems can be avoided by depending on cyclones. As a result, we can identify research problems with regard to gas purification from dust through:

1. Gas analyses and control of the proportions of the raw materials being used in the cement industry and their homogenization process to obtain a high-specification product free from dust and volatile clinker particles, which is in the interests of the heat recovery project.
2. Purifying hot gases from dust and small particles of clinker by creating vortices of hot gases using a cyclone separator operating in a centrifugal system followed by collecting them and returning them to the raw materials silo.
3. Since the boiler is divided into three parts (the economizer, evaporator and overheated), the tubes of the first part of the boiler, which is overheated, must be chosen from resistant metal friction and high temperatures.
4. Periodic monitoring of boiler performance by checking the pressures at the boiler entrance and the temperatures of the produced steam.

PART 3

METHODOLOGY

This chapter discusses the different cogeneration systems that can be used in cement plants. These cogeneration systems can generate energy approximately 30 - 40% of the energy spent on cement production. Some assumptions were made to get the system's net performance and power simulations according to references[50,51,52,44]:

1. The system equipment is isolated from the environment, and there is no heat transfer.
2. The liquid leaves the condenser in a saturated state.
3. Neglecting the pressure drop in the boiler tubes and condenser.
4. Considering the system working in a stable state by neglecting kinetic energy, potential energy, friction in the system, and heat loss.
5. The dead state temperature and pressure are assumed to be $T_0 = 25\text{ }^\circ\text{C}$ and $P_0 = 101.325\text{ kPa}$.

3.1. THERMODYNAMIC ANALYSIS AND SIMULATION SCHEME FOR ORGANIC RANKINE CYCLE

The Organic Rankine cycle is considered to be less than the ORC to treatment with the waste heat recovery. In this work, R123 was used as the working fluid to achieve the simulation of the ORC. Figure 3.9 shows the ORC in the cement factory. The feed pump delivers the fluid into two branches. One line proceeds towards the AQC boiler; here, the working fluid should be preheated, vaporized, and superheated. The other line enters the SP boiler with the fluid in the same process being preheated, vaporized, and superheated. The two-stream collects in the turbine to obtain the power. After that, the stream goes to the condenser and is finally sent to the pump.

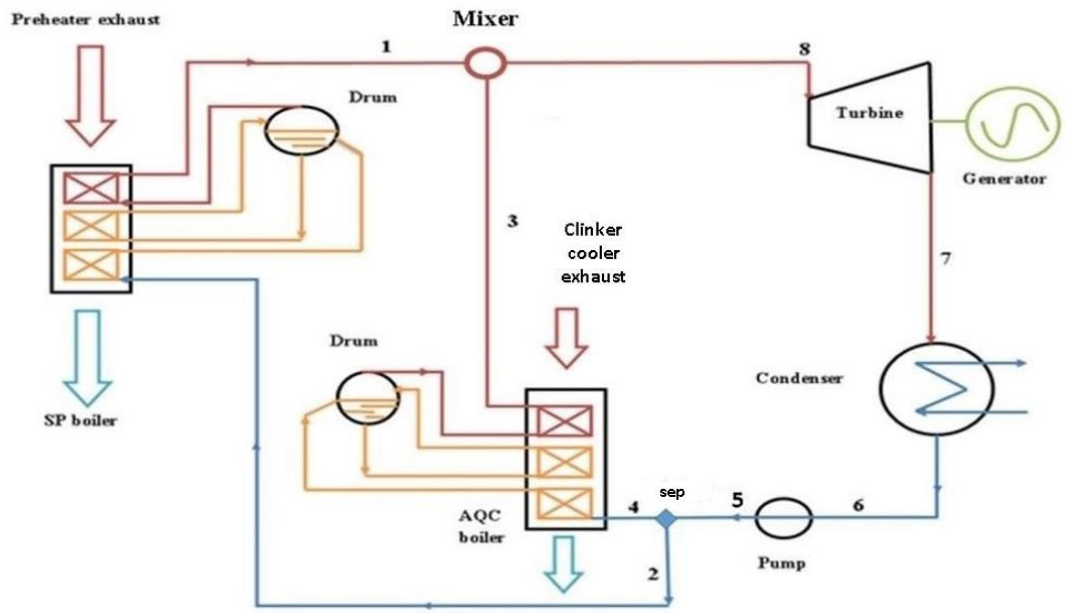


Figure 3.1. Organic Rankine cycle at the cement plant.

3.1.1. Pump Parameter

The principal aim of the use of the pumps in the cogeneration system is to increase the pressure of the steam before it enters the turbine to enhance the increase of the specific power. The pumping process is assumed to be reversible and adiabatic, i.e.; isentropic. The inputs to the pump model are the atmospheric pressure and ambient temperature. The mass, energy, and exergy balances are applied to get the pump parameters [53]:

$$\dot{m}_5 = \dot{m}_6 \quad (3.1)$$

$$\dot{W}_p = \dot{m}_6(h_5 - h_6) \quad (3.2)$$

$$\eta_p = \frac{(h_{5s} - h_6)}{(h_5 - h_6)} \quad (3.3)$$

$$\dot{E}X_6 = \dot{m}_6(h_6 - h_0 - T_0(s_6 - s_0)) \quad (3.4)$$

$$\dot{E}d_p = \dot{E}X_6 - \dot{E}X_5 + \dot{W}_p \quad (3.5)$$

$$\dot{E}d_p \% = (\dot{E}d_p / \dot{E}d_{Total}) * 100 \quad (3.6)$$

3.1.2. Turbine Parameter

The turbine, which is a rotating device connected to the electric generator, converts the thermal energy resulting from steam pressure into mechanical energy. The mass, energy, and exergy balances are applied to get the turbine parameters [54].

$$\dot{m}_8 = \dot{m}_7 \quad (3.7)$$

$$\dot{W}_T = \dot{m}_8(h_8 - h_7) \quad (3.8)$$

$$\dot{E}X_8 = \dot{m}_8(h_8 - h_0 - T_0(s_8 - s_0)) \quad (3.9)$$

$$\eta_T = \frac{(h_8 - h_7)}{(h_8 - h_{7s})} \quad (3.10)$$

$$\dot{E}d_T = \dot{E}X_8 - \dot{E}X_7 - \dot{W}_T \quad (3.11)$$

$$\dot{E}d_T\% = (\dot{E}d_T/\dot{E}d_{Total}) * 100 \quad (3.12)$$

3.2.3. Condenser Parameter

The steam coming from the turbine enters the condenser from the top after losing much of its pressure and temperature. The cooling water enters the spiral tubes from the bottom of the condenser, and then an exchange occurs between the steam and the spiral tubes, turning the steam into water. This water is returned to the boilers through special pumps. The mass, energy, and exergy balances are applied to get the condenser parameters [55]:

$$\dot{m}_7 = \dot{m}_6 \quad (3.13)$$

$$\dot{Q}_{con} = \dot{m}_7(h_7 - h_6) \quad (3.14)$$

$$\dot{E}X_{con} = \dot{m}_7(h_7 - h_0 - T_0(s_7 - s_0)) \quad (3.15)$$

$$\dot{E}d_{con} = \dot{E}X_{con} - \dot{E}X_6 \quad (3.16)$$

$$\dot{E}d_{con}\% = (\dot{E}d_{con}/\dot{E}d) * 100 \quad (3.17)$$

3.1.4. Mixer Parameter

The two streams of steam produced from the AQC boiler and the SP boiler are mixed in the mixing chamber before entering the turbine. Assuming that the mixture is adiabatic. To get the parameters of the mixture, the following equation is applied [56]:

$$\dot{m}_1 + \dot{m}_3 = \dot{m}_8 \quad (3.18)$$

$$\dot{m}_1 h_1 + \dot{m}_3 h_3 = \dot{m}_8 h_8 \quad (3.19)$$

$$\dot{E}X_1 = \dot{m}_1(h_1 - h_0 - T_0(s_1 - s_0)) \quad (3.20)$$

$$\dot{E}X_3 = \dot{m}_3(h_3 - h_0 - T_0(s_3 - s_0)) \quad (3.21)$$

$$\dot{E}d_{mix} = \dot{E}X_1 + \dot{E}X_3 - \dot{E}X_8 \quad (3.22)$$

$$\dot{E}d_{mix} \% = (\dot{E}d_{mix} / \dot{E}d_{Total}) * 100 \quad (3.23)$$

3.1.5. Separator Parameter

The mass, energy, and exergy analysis of the separator can be summarized as[57]:

$$\dot{m}_5 = \dot{m}_2 + \dot{m}_4 \quad (3.24)$$

$$\dot{m}_4 h_4 = \dot{m}_2 h_2 + \dot{m}_4 h_4 \quad (3.25)$$

$$\dot{E}X_2 = \dot{m}_1(h_2 - h_0 - T_0(s_2 - s_0)) \quad (3.26)$$

$$\dot{E}X_4 = \dot{m}_4(h_4 - h_0 - T_0(s_4 - s_0)) \quad (3.27)$$

$$\dot{E}d_{sep} = \dot{E}X_5 - \dot{E}X_2 - \dot{E}X_4 \quad (3.28)$$

$$\dot{E}d_{sep} \% = (\dot{E}d_{sep} / \dot{E}d_{Total}) * 100 \quad (3.29)$$

3.1.6. AQC Boiler Parameter

This type of boiler is used with the clinker cooler. The cold air from the environment through the cooling fans enters the grid cooler to cool the clinker produced in the rotary kiln. Then, it is released into the air, carrying with it the temperature of the clinker. To get the parameters of the AQC boiler, the following equation is applied: The mass, energy, and exergy analysis of the AQC boiler can be summarized as [44]:

$$\dot{m}_4 = \dot{m}_3 \quad (3.30)$$

$$\dot{Q}_{AQC} = \dot{m}_4(h_3 - h_4) \quad (3.31)$$

$$\dot{Q}_{AQC} = \dot{m}_{\text{air}} * C_{P,\text{air}}(T_{\text{in,air}} - T_{\text{out,air}}) \quad (3.32)$$

$$\dot{E}X_{\text{in,AQC}} = \dot{m}_{\text{air}} [h_{\text{in,air}} - h_{\text{amb,air}} - T_0(s_{\text{in,air}} - s_{\text{amb,air}})] \quad (3.33)$$

$$\dot{E}X_{\text{out,AQC}} = \dot{m}_{\text{air}} [h_{\text{out,air}} - h_{\text{amb,air}} - T_0(s_{\text{out,air}} - s_{\text{amb,air}})] \quad (3.34)$$

$$\dot{E}d_{AQC} = \dot{E}X_{\text{in,SP}} - \dot{E}X_{\text{out,SP}} + \dot{E}X_4 - \dot{E}X_3 \quad (3.35)$$

$$\dot{E}d_{AQC}\% = (\dot{E}d_{AQC}/\dot{E}d_{\text{Total}}) * 100 \quad (3.36)$$

The enthalpy, entropy, and constant specific heat of the air per unit mole can be determined by dividing the preceding equations by the molar mass of the air[58].

$$\bar{h}_a = \sum_{i=1}^k y_i \bar{h}_i \quad (3.37)$$

$$\bar{s}_a = \sum_{i=1}^k y_i \bar{s}_i \quad (3.38)$$

$$\bar{c}_{p,a} = \sum_{i=1}^k y_i \bar{c}_{p,i} \quad (3.39)$$

Where y_i is the molar fraction of the O₂ and N₂. The molar mass of the air is calculated by using the following equation [58]:

$$M_a = \sum_{i=1}^k y_i M_i \quad (3.40)$$

3.1.7. SP Boiler Parameter

This boiler is used at the reheating in the cement plant. The function of this tower is to heat the raw materials used in the production of cement before entering the rotary kiln using part of this heat generated in the kiln and the rest of the heat exiting into the atmosphere. The amount of heat that is released to the ambient can be used in the

cogeneration cycle. The mass, energy, and exergy analysis of the SP boiler can be summarized as [59]:

$$\dot{m}_2 = \dot{m}_1 \quad (3.41)$$

$$\dot{Q}_{SP} = \dot{m}_2(h_1 - h_2) \quad (3.42)$$

$$\dot{E}X_{in_{SP}} = \dot{m}_{ex,g} \left[h_{in_{gas}} - h_{amb_{ex,gas}} - T_0 (s_{in_{ex,g}} - s_{amb_{ex,g}}) \right] \quad (3.43)$$

$$\dot{E}X_{out_{SP}} = \dot{m}_{ex,g} [h_{out_{ex,g}} - h_{amb_{ex,g}} - T_0 (s_{out_{ex,g}} - s_{amb_{ex,g}})] \quad (3.44)$$

$$\dot{E}d_{SP} = \dot{E}X_{in_{SP}} - \dot{E}X_{out_{SP}} + \dot{E}X_2 - \dot{E}X_1 \quad (3.45)$$

$$\dot{E}d_{SP} \% = (\dot{E}d_{SP} / \dot{E}d_{Total}) * 100 \quad (3.46)$$

The enthalpy, entropy, and constant specific heat of the exhaust gases per unit mole of the exhaust gases can be determined by dividing the preceding equations by the molar mass of the exhaust gases [58].

$$\bar{h}_{ex,g} = \sum_{i=1}^k y_i \bar{h}_i \quad (3.47)$$

$$\bar{s}_{ex,g} = \sum_{i=1}^k y_i \bar{s}_i \quad (3.48)$$

$$\bar{c}_{p,ex,g} = \sum_{i=1}^k y_i \bar{c}_{p,i} \quad (3.49)$$

Where y_i is the molar fraction of the exhaust gases. The molar mass of the exhaust gases is calculated by using the following equation [58]:

$$M_{ex,g} = \sum_{i=1}^k y_i M_i \quad (3.50)$$

The amount of heat used in the cogeneration cycle is determined as:

$$\dot{Q}_{SP} = \dot{m}_{ex,g} * C_{p_{ex,g}} (T_{in_{ex,g}} - T_{out_{ex,g}}) \quad (3.51)$$

3.1.8. Drum

The drum has two primary functions: it receives heated feed water to make up for water that's converted to steam and flows out of the boiler. It also collects the steam that has produced in the water.

3.1.9. ORC Performance

Net power output, plant efficiency, and plant exergy for the ORC system is calculated from the following equations [60]:

$$\dot{W}_{net} = \dot{W}_T - \dot{W}_p \quad (3.52)$$

$$\eta_{th} = \dot{W}_{net} / (\dot{Q}_{AQC} + \dot{Q}_{SP}) \quad (3.53)$$

$$\eta_{EX} = \dot{W}_{net} / (\dot{E}X_{inAQC} + \dot{E}X_{inSP}) \quad (3.54)$$

3.2. THERMODYNAMIC ANALYSIS AND SIMULATION SCHEME FOR STEAM CYCLE WITH SINGLE FLASH

The steam in the pressure lowered case can be separated from the water-saturated cycle, called the single flash steam power cycle. The initial pressure of the flasher tank and the final pressure affect the amount of flashing steam. The drop of pressure is inversely proportional to the amount of steam in the flashing tank. In contrast, the low-pressure steam decreases the power. In other words, the amount of steam increases as the pressure in the vapor decreases, so less energy is generated. Figure 3.10 presents the concept of recovering the waste heat in the cement plant through a single flash steam cycle. The cycle concept is for the feed pump to send the working fluid to the AQC boiler to heat the fluid initially, take one part of it, and send it to the flasher to separate the saturated steam and saturated water. Saturated steam is sent to the turbine to generate power but in a small percentage. The remaining preheated working fluid continues to be heated in the AQC boiler and the other part of the preheated working fluid is sent to the SP boiler for further heating. The two-stream coming from the AQC and SP boilers meet, mix and pass through the turbine to produce power. When the working fluid exits the turbine, it expands in the flasher to separate it into saturated

water and saturated steam. The saturated vapor is sent to the turbine for power generation. The turbine exhaust enters the condenser to condense, then is sent to the pump to mix with dripping water from the flasher.

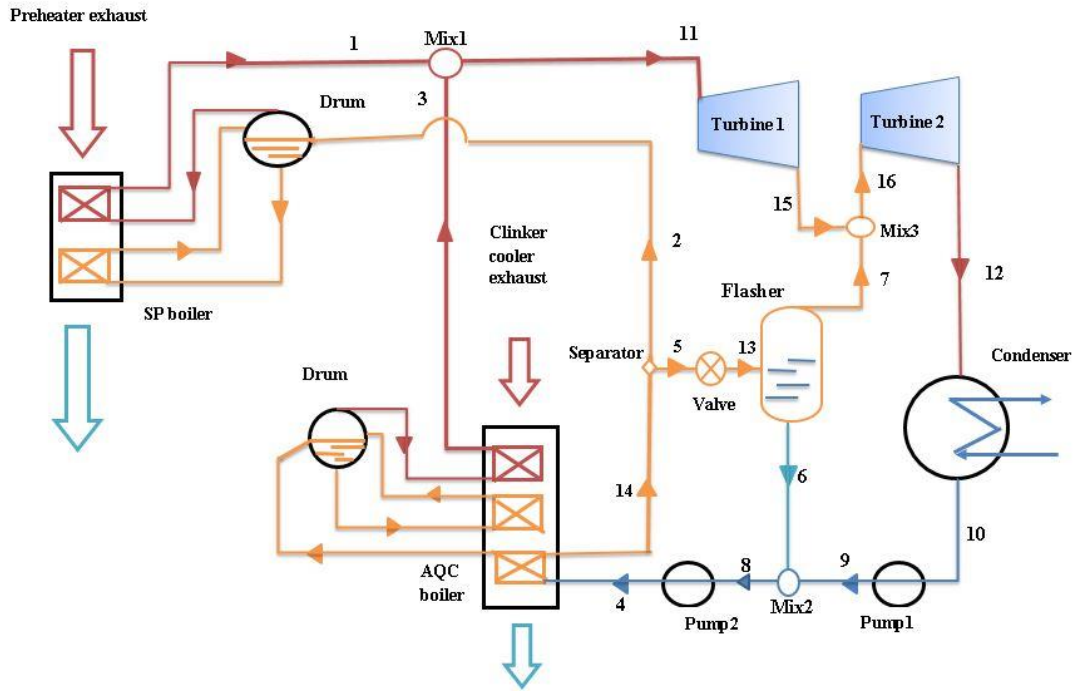


Figure 3.2. Steam cycle with a single flash.

3.2.1. Pumps Parameter

The mass, energy, and exergy analysis for Pump1 is determined from the following equations [53]:

$$\dot{m}_{10} = \dot{m}_9 \quad (3.55)$$

$$\dot{W}_{P_1} = \dot{m}_{10}(h_9 - h_{10}) \quad (3.56)$$

$$\dot{E}X_{10} = \dot{m}_{10}(h_{10} - h_0 - T_0(s_{10} - s_0)) \quad (3.57)$$

$$\dot{E}d_{P_1} = \dot{E}X_{10} - \dot{E}X_9 + \dot{W}_{P_1} \quad (3.58)$$

$$\dot{E}d_{P_1} \% = (\dot{E}d_{P_1} / \dot{E}d_{Total}) * 100 \quad (3.59)$$

The mass, energy, and exergy analysis for Pump2 is determined from the following equations:

$$\dot{m}_8 = \dot{m}_4 \quad (3.60)$$

$$\dot{W}_{P_2} = \dot{m}_4(h_4 - h_8) \quad (3.61)$$

$$\dot{E}X_8 = \dot{m}_8(h_8 - h_0 - T_0(s_8 - s_0)) \quad (3.62)$$

$$\dot{E}d_{P_2} = \dot{E}X_8 - \dot{E}X_4 + \dot{W}_{P_2} \quad (3.63)$$

$$\dot{E}d_{P_2}\% = (\dot{E}d_{P_2}/\dot{E}d_{Total}) * 100 \quad (3.64)$$

3.2.2. Turbines Parameter

The mass, energy, and exergy analysis for the turbine 1 is calculated from the following equations [56,61]:

$$\dot{m}_{11} = \dot{m}_{15} \quad (3.65)$$

$$\dot{W}_{T1} = \dot{m}_{11}(h_{11} - h_{15}) \quad (3.66)$$

$$\dot{E}X_{11} = \dot{m}_{11}(h_{11} - h_0 - T_0(s_{11} - s_0)) \quad (3.67)$$

$$\dot{E}X_{15} = \dot{m}_{15}(h_{15} - h_0 - T_0(s_{15} - s_0))$$

$$\dot{E}d_{T1} = \dot{E}X_{11} - \dot{E}X_{15} - \dot{W}_{T1} \quad (3.68)$$

$$\dot{E}d_{T1}\% = (\dot{E}d_{T1}/\dot{E}d_{Total}) * 100 \quad (3.69)$$

The mass, energy, and exergy analysis for the turbine 2 is calculated from the following equations:

$$\dot{m}_{16} = \dot{m}_{12} \quad (3.70)$$

$$\dot{W}_{T2} = \dot{m}_{16}(h_{16} - h_{12}) \quad (3.71)$$

$$\dot{E}X_{16} = \dot{m}_{16}(h_{16} - h_0 - T_0(s_{16} - s_0)) \quad (3.72)$$

$$\dot{E}d_{T2} = \dot{E}X_{16} + \dot{E}X_{12} - \dot{W}_{T2} \quad (3.73)$$

$$\dot{E}d_{T2}\% = (\dot{E}d_{T2}/\dot{E}d_{Total}) * 100 \quad (3.74)$$

3.2.3. Condenser Parameter

The mass, energy, and exergy analysis for the condenser is determined from the following equations [55]:

$$\dot{m}_{12} = \dot{m}_{10} \quad (3.75)$$

$$\dot{Q}_{con} = \dot{m}_{12}(h_{12} - h_{10}) \quad (3.76)$$

$$\dot{E}X_{12} = \dot{m}_{12}(h_{12} - h_0 - T_0(s_{12} - s_0)) \quad (3.77)$$

$$\dot{E}d_{12} = \dot{E}X_{12} - \dot{E}X_{10} \quad (3.78)$$

$$\dot{E}d_{con}\% = (\dot{E}d_{con}/\dot{E}d_{Total}) * 100 \quad (3.79)$$

3.2.4. Flasher Parameter

The primary aim of the flash of the cycle is to separate the steam produced in the boiler from the water. Steam is spent on the turbine to generate power, and the water is returned to the pump to be pumped to the boiler. To get the parameters of the turbine, the following equation is applied [62]:

$$\dot{m}_5 = \dot{m}_6 + \dot{m}_7 \quad (3.80)$$

$$\dot{m}_5 h_5 = \dot{m}_6 h_6 + \dot{m}_7 h_7 \quad (3.81)$$

$$\dot{E}X_5 = \dot{m}_5(h_5 - h_0 - T_0(s_5 - s_0)) \quad (3.82)$$

$$\dot{E}X_6 = \dot{m}_6(h_6 - h_0 - T_0(s_6 - s_0)) \quad (3.83)$$

$$\dot{E}X_7 = \dot{m}_7(h_7 - h_0 - T_0(s_7 - s_0)) \quad (3.84)$$

$$\dot{E}d_{flash} = \dot{E}X_5 - \dot{E}X_6 - \dot{E}X_7 \quad (3.85)$$

$$\dot{E}d_{flash}\% = (\dot{E}d_{flash}/\dot{E}d_{Total}) * 100 \quad (3.86)$$

3.2.5. Mixers Parameter

The mass, energy, and exergy analysis for mixer1 is determined from the following equations [56]:

$$\dot{m}_1 + \dot{m}_3 = \dot{m}_{11} \quad (3.87)$$

$$\dot{m}_1 h_1 + \dot{m}_3 h_3 = \dot{m}_{11} h_{11} \quad (3.88)$$

$$\dot{E}X_1 = \dot{m}_1(h_1 - h_0 - T_0(s_1 - s_0)) \quad (3.89)$$

$$\dot{E}X_3 = \dot{m}_3(h_3 - h_0 - T_0(s_3 - s_0)) \quad (3.90)$$

$$\dot{E}X_{11} = \dot{m}_{11}(h_{11} - h_0 - T_0(s_{11} - s_0)) \quad (3.91)$$

$$\dot{E}d_{mix1} = \dot{E}X_1 + \dot{E}X_3 - \dot{E}X_{11} \quad (3.92)$$

$$\dot{E}d_{mix1}\% = (\dot{E}d_{mix1}/\dot{E}d_{Total}) * 100 \quad (3.93)$$

The mass, energy, and exergy analysis for mixer 2 is determined from the following equations:

$$\dot{m}_6 + \dot{m}_9 = \dot{m}_8 \quad (3.94)$$

$$\dot{m}_6 h_6 + \dot{m}_9 h_9 = \dot{m}_8 h_8 \quad (3.95)$$

$$\dot{E}X_6 = \dot{m}_6(h_6 - h_0 - T_0(s_6 - s_0)) \quad (3.96)$$

$$\dot{E}X_9 = \dot{m}_9(h_9 - h_0 - T_0(s_9 - s_0)) \quad (3.97)$$

$$\dot{E}X_8 = \dot{m}_8(h_8 - h_0 - T_0(s_8 - s_0)) \quad (3.98)$$

$$\dot{E}d_{mix2} = \dot{E}X_6 + \dot{E}X_9 - \dot{E}X_8 \quad (3.99)$$

$$\dot{E}d_{mix2}\% = (\dot{E}d_{mix2}/\dot{E}d_{Total}) * 100 \quad (3.100)$$

The mass, energy, and exergy analysis for mixer 3 is determined from the following equations:

$$\dot{m}_{15} + \dot{m}_7 = \dot{m}_{16} \quad (3.101)$$

$$\dot{m}_{15} h_{15} + \dot{m}_7 h_7 = \dot{m}_{16} h_{16} \quad (3.102)$$

$$\dot{E}d_{mix3} = \dot{E}X_{15} + \dot{E}X_7 - \dot{E}X_{16} \quad (3.103)$$

$$\dot{E}d_{mix3}\% = (\dot{E}d_{mix3}/\dot{E}d_{Total}) * 100 \quad (3.104)$$

3.2.6. Separator Parameter

The separator is used to split the fluid into two streams towards the AQC and LSP boilers. The mass, energy, and exergy analysis of the separator can be summarized as [62]:

$$\dot{m}_{14} = \dot{m}_2 + \dot{m}_5 \quad (3.105)$$

$$\dot{m}_{14} h_{14} = \dot{m}_2 h_2 + \dot{m}_5 h_5 \quad (3.106)$$

$$\dot{E}X_2 = \dot{m}_2(h_2 - h_0 - T_0(s_2 - s_0)) \quad (3.107)$$

$$\dot{E}X_5 = \dot{m}_5(h_5 - h_0 - T_0(s_5 - s_0)) \quad (3.108)$$

$$\dot{E}X_{14} = \dot{m}_{14}(h_{14} - h_0 - T_0(s_{14} - s_0)) \quad (3.109)$$

$$\dot{E}d_{sep} = \dot{E}X_{13} - \dot{E}X_5 - \dot{E}X_2 \quad (3.110)$$

$$\dot{E}d_{sep}\% = (\dot{E}d_{sep}/\dot{E}d_{Total}) * 100 \quad (3.111)$$

3.2.7. Valve Parameters

$$\dot{m}_5 = \dot{m}_{13} \quad (3.112)$$

$$h_4 = h_{13} \quad (3.113)$$

$$\dot{E}X_{13} = \dot{m}_{14}(h_{13} - h_0 - T_0(s_{13} - s_0)) \quad (3.114)$$

$$\dot{E}d_{valve} = \dot{E}X_5 - \dot{E}X_{13} \quad (3.115)$$

$$\dot{E}d_{valve}\% = (\dot{E}d_{div}/\dot{E}d_{Total}) * 100 \quad (3.116)$$

3.2.8. AQC Boiler Parameter

The mass, energy, and exergy analysis of the AQC boiler can be summarized as [54]:

$$\dot{m}_4 = \dot{m}_{14} + \dot{m}_3 \quad (3.117)$$

$$\dot{Q}_{AQC} = \dot{m}_{14}(h_{14} - h_4) + \dot{m}_3(h_3 - h_4) \quad (3.118)$$

$$\dot{E}X_{inSP} = \dot{m}_{ex,g} [h_{in,gas} - h_{amb,ex,gas} - T_0 (s_{in,ex,g} - s_{amb,ex,g})] \quad (3.119)$$

$$\dot{E}X_{outSP} = \dot{m}_{ex,g} [h_{out,ex,g} - h_{amb,ex,g} - T_0 (s_{out,ex,g} - s_{amb,ex,g})] \quad (3.120)$$

$$\dot{E}d_{AQC} = \dot{E}X_{inSP} - \dot{E}X_{outSP} + \dot{E}X_4 - \dot{E}X_{14} + \dot{E}X_3 \quad (3.121)$$

$$\dot{E}d_{AQC}\% = (\dot{E}d_{AQC}/\dot{E}d_{Total}) * 100 \quad (3.122)$$

3.2.9. SP Boiler Parameter

The mass, energy, and exergy analysis of the SP boiler can be summarized as [54]:

$$\dot{m}_3 = \dot{m}_1 \quad (3.123)$$

$$\dot{Q}_{SP} = \dot{m}_3(h_1 - h_3) \quad (3.124)$$

$$\dot{E}X_{inSP} = \dot{m}_{ex,g} [h_{in,gas} - h_{amb,ex,gas} - T_0 (s_{in,ex,g} - s_{amb,ex,g})] \quad (3.125)$$

$$\dot{E}X_{outSP} = \dot{m}_{ex,g} [h_{outex,g} - h_{ambex,g} - T_0 (s_{outex,g} - s_{ambex,g})] \quad (3.126)$$

$$\dot{E}d_{SP} = \dot{E}X_{inSP} - \dot{E}X_{outSP} + \dot{E}X_3 - \dot{E}X_1 \quad (3.127)$$

$$\dot{E}d_{SP}\% = (\dot{E}d_{SP}/\dot{E}d_{Total}) * 100 \quad (3.128)$$

3.2.10. Single Flash Cycle Performance

Net power output, plant efficiency, and plant exergy for the steam cycle with a single flash is calculated from the following equations [62]:

$$\dot{W}_{net} = \dot{W}_{T1} + \dot{W}_{T2} - \dot{W}_{P1} - \dot{W}_{P2} \quad (3.129)$$

$$\eta_{th} = \dot{W}_{net}/(\dot{Q}_{AQC} + \dot{Q}_{SP}) \quad (3.130)$$

$$\eta_{EX} = \dot{W}_{net}/(\dot{E}X_{inAQC} + \dot{E}X_{inSP}) \quad (3.131)$$

3.3. THERMODYNAMIC ANALYSIS AND SIMULATION SCHEME FOR STEAM CYCLE WITH DUAL PRESSURE

The steam cycle with dual pressure is better than single pressure, especially at low and medium temperatures of preheater waste heat and clinker coolant air hot. Figure 3.11 shows the double pressure stream cycle in the cement plant. After preheating, a low-pressure feed pump allows the working fluid to pass through and then be sent to the AQC boiler. For power generation, part of which is power by the turbine, the turbine receives the low-pressure steam generated by the AQC boiler by evaporating and heating a portion of the preheated working fluid. The high-pressure pump is used to pass another part of the preheated working fluid, which then evaporates and is intensively heated through the AQC boiler. A high-pressure pump is used to receive the remaining preheated working fluid, which is sent afterwards to the SP boiler in a state of steaming and heating. The turbine generates power by mixed reception of two streams of high-pressure ultra-heated steam from an AQC and SP boiler. A low-pressure feed pump receives the turbine exhaust after it is condensed.

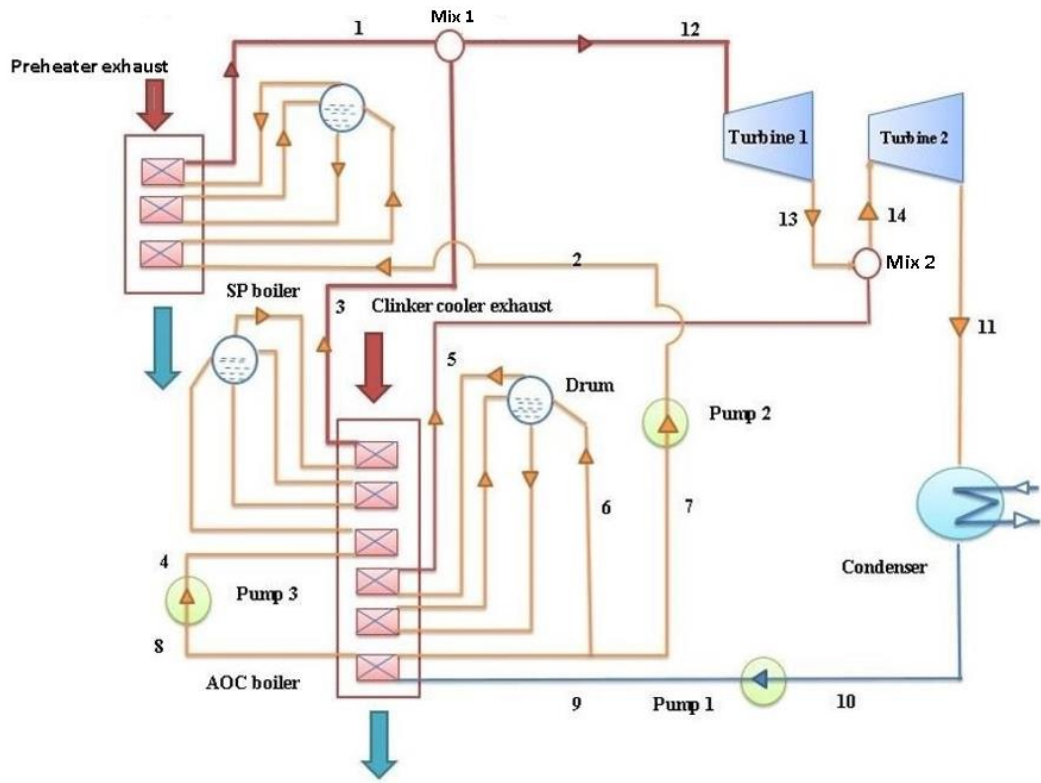


Figure 3.3. Dual steam cycle at the cement plant.

3.3.1. Pumps Parameter

The mass, energy, and exergy analysis for pump 1 is determined from the following equations [54][63]:

$$\dot{m}_{10} = \dot{m}_9 \quad (3.132)$$

$$\dot{W}_{P_1} = \dot{m}_{10}(h_9 - h_{10}) \quad (3.133)$$

$$\dot{E}X_{10} = \dot{m}_{10}(h_{10} - h_0 - T_0(s_{10} - s_0)) \quad (3.134)$$

$$\dot{E}d_{P_1} = \dot{E}X_{10} - \dot{E}X_9 + \dot{W}_{P_1} \quad (3.135)$$

$$\dot{E}d_{P_1}\% = (\dot{E}d_{P_1}/\dot{E}d_{Total}) * 100 \quad (3.136)$$

Also, the mass, energy, and exergy analysis for pump 2 is determined from the following equations:

$$\dot{m}_7 = \dot{m}_2 \quad (3.137)$$

$$\dot{W}_{P_2} = \dot{m}_7(h_2 - h_7) \quad (3.138)$$

$$\dot{E}X_2 = \dot{m}_2(h_2 - h_0 - T_0(s_2 - s_0)) \quad (3.139)$$

$$\dot{E}d_{P_2} = \dot{E}X_2 - \dot{E}X_7 + \dot{W}_{P_2} \quad (3.140)$$

$$\dot{E}d_{P_2}\% = (\dot{E}d_{P_2}/\dot{E}d_{Total}) * 100 \quad (3.141)$$

The mass, energy, and exergy analysis for pump 3 is determined from the following equations:

$$\dot{m}_4 = \dot{m}_8 \quad (3.142)$$

$$\dot{W}_{P_3} = \dot{m}_8(h_4 - h_8) \quad (3.143)$$

$$\dot{E}X_4 = \dot{m}_4(h_4 - h_0 - T_0(s_4 - s_0)) \quad (3.144)$$

$$\dot{E}d_{P_3} = \dot{E}X_8 - \dot{E}X_4 + \dot{W}_{P_3} \quad (3.145)$$

$$\dot{E}d_{P_3}\% = (\dot{E}d_{P_3}/\dot{E}d_{Total}) * 100 \quad (3.146)$$

3.3.2. Turbines Parameter

The mass, energy, and exergy analysis for the turbine 1 is determined from the following equations [54] [63]:

$$\dot{m}_{12} = \dot{m}_{13} \quad (3.147)$$

$$\dot{W}_{T1} = \dot{m}_{12}(h_{12} - h_{13}) \quad (3.148)$$

$$\dot{E}X_{13} = \dot{m}_{13}(h_{13} - h_0 - T_0(s_{13} - s_0)) \quad (3.149)$$

$$\dot{E}d_{T1} = \dot{E}X_{12} - \dot{E}X_{13} - \dot{W}_{T1} \quad (3.150)$$

$$\dot{E}d_{T1}\% = (\dot{E}d_{T1}/\dot{E}d_{Total}) * 100 \quad (3.151)$$

The mass, energy, and exergy analysis for the turbine 2 is determined from the following equations:

$$\dot{m}_{14} = \dot{m}_{11} \quad (3.152)$$

$$\dot{W}_{T2} = \dot{m}_{14}(h_{14} - h_{11}) \quad (3.153)$$

$$\dot{E}X_{14} = \dot{m}_{14}(h_{14} - h_0 - T_0(s_{14} - s_0)) \quad (3.154)$$

$$\dot{E}d_{T2} = \dot{E}X_{14} - \dot{E}X_{11} - \dot{W}_{T2} \quad (3.155)$$

$$\dot{E}d_{T2}\% = (\dot{E}d_{T2}/\dot{E}d_{Total}) * 100 \quad (3.156)$$

3.3.3. Condenser Parameter

The mass, energy, and exergy analysis for the condenser is determined from the following equations [55]:

$$\dot{m}_{11} = \dot{m}_{10} \quad (3.157)$$

$$\dot{Q}_{con} = \dot{m}_{11}(h_{11} - h_{10}) \quad (3.158)$$

$$\dot{E}X_{11} = \dot{m}_{11}(h_{11} - h_0 - T_0(s_{11} - s_0)) \quad (3.159)$$

$$\dot{E}d_{11} = \dot{E}X_{11} - \dot{E}X_{10} \quad (3.160)$$

$$\dot{E}d_{con}\% = (\dot{E}d_{con}/\dot{E}d_{Total}) * 100 \quad (3.161)$$

3.3.4. Mixers Parameter

The mass, energy, and exergy analysis for the mixer1 is determined from the following equations [56]:

$$\dot{m}_1 + \dot{m}_3 = \dot{m}_{12} \quad (3.162)$$

$$\dot{m}_1 h_1 + \dot{m}_3 h_3 = \dot{m}_{12} h_{12} \quad (3.163)$$

$$\dot{E}X_1 = \dot{m}_1(h_1 - h_0 - T_0(s_1 - s_0)) \quad (3.164)$$

$$\dot{E}X_3 = \dot{m}_3(h_3 - h_0 - T_0(s_3 - s_0)) \quad (3.165)$$

$$\dot{E}X_{12} = \dot{m}_{12}(h_{12} - h_0 - T_0(s_{12} - s_0)) \quad (3.166)$$

$$\dot{E}d_{mix\ 1} = \dot{E}X_1 + \dot{E}X_3 - \dot{E}X_{12} \quad (3.167)$$

$$\dot{E}d_{mix\ 1}\% = (\dot{E}d_{mix\ 1}/\dot{E}d_{Total}) * 100 \quad (3.168)$$

The mass, energy, and exergy analysis for the mixer 2 is calculated from the following equations:

$$\dot{m}_{13} + \dot{m}_5 = \dot{m}_{14} \quad (3.169)$$

$$\dot{m}_{13} h_{13} + \dot{m}_5 h_5 = \dot{m}_{14} h_{14} \quad (3.170)$$

$$\dot{E}X_5 = \dot{m}_5(h_5 - h_0 - T_0(s_5 - s_0)) \quad (3.171)$$

$$\dot{E}d_{mix\ 2} = \dot{E}X_{13} + \dot{E}X_5 - \dot{E}X_{14} \quad (3.172)$$

$$\dot{E}d_{mix\ 2}\% = (\dot{E}d_{mix\ 2}/\dot{E}d_{Total}) * 100 \quad (3.173)$$

3.3.5. AQC Boiler Parameter

The mass, energy, and exergy analysis of the SP boiler can be summarized as [54]:

$$\dot{m}_9 = \dot{m}_7 + \dot{m}_3 + \dot{m}_5 \quad (3.174)$$

$$\dot{Q}_{AQC} = \dot{m}_9(h_8 - h_9) + \dot{m}_3(h_3 - h_4) + (\dot{m}_9 - \dot{m}_7 - \dot{m}_8)(h_5 - h_6) \quad (3.175)$$

$$\dot{E}X_{inSP} = \dot{m}_{ex,g} [h_{in,gas} - h_{amb_{ex,gas}} - T_0 (s_{in_{ex,g}} - s_{amb_{ex,g}})] \quad (3.176)$$

$$\dot{E}X_{outSP} = \dot{m}_{ex,g} [h_{out_{ex,g}} - h_{amb_{ex,g}} - T_0 (s_{out_{ex,g}} - s_{amb_{ex,g}})] \quad (3.177)$$

$$\dot{E}d_{AQC} = \dot{E}X_{inSP} - \dot{E}X_{outSP} + \dot{E}X_9 - \dot{E}X_3 - \dot{E}X_5 - \dot{E}X_7 \quad (3.178)$$

$$\dot{E}d_{AQC}\% = (\dot{E}d_{AQC}/\dot{E}d_{Total}) * 100 \quad (3.179)$$

3.3.6. SP Boiler Parameter

The mass, energy, and exergy analysis of the SP boiler can be summarize as:

$$\dot{m}_2 = \dot{m}_1 \quad (3.180)$$

$$\dot{Q}_{SP} = \dot{m}_3(h_1 - h_2) \quad (3.181)$$

$$\dot{E}X_{inSP} = \dot{m}_{ex,g} [h_{in,gas} - h_{amb_{ex,gas}} - T_0 (s_{in_{ex,g}} - s_{amb_{ex,g}})] \quad (3.181)$$

$$\dot{E}X_{outSP} = \dot{m}_{ex,g} [h_{out_{ex,g}} - h_{amb_{ex,g}} - T_0 (s_{out_{ex,g}} - s_{amb_{ex,g}})] \quad (3.182)$$

$$\dot{E}d_{SP} = \dot{E}X_{inSP} - \dot{E}X_{outSP} + \dot{E}X_2 - \dot{E}X_1 \quad (3.183)$$

$$\dot{E}d_{SP}\% = (\dot{E}d_{SP}/\dot{E}d_{Total}) * 100 \quad (3.184)$$

3.3.7. Dual Steam Cycle Performance

Net power output, plant efficiency, and plant exergy for the dual steam cycle is calculated from the following equations [65]:

$$\dot{W}_{net} = \dot{W}_{T1} + \dot{W}_{T2} - \dot{W}_{P1} - \dot{W}_{P2} - \dot{W}_{P3} \quad (3.185)$$

$$\eta_{th} = \dot{W}_{net} / (\dot{Q}_{AQC} + \dot{Q}_{SP}) \quad (3.186)$$

$$\eta_{EX} = \dot{W}_{net} / (\dot{E}X_{inAQC} + \dot{E}X_{inSP}) \quad (3.187)$$

3.4. COGENERATION SYSTEMS INPUT PARAMETER

Table 3.1. Input parameter for cogeneration systems [55,44,58].

Isentropic Efficiency of Turbines (%)	88
Pressure of Environment (MPa)	0.10135
Temperature of Environment (°C)	25
Isentropic Efficiency of Pump (%)	75
Turbine Exhaust Dryness Percentage (%)	90
Temperature Difference at an Approach Point (°C)	5
Temperature Difference at a Pinch Point (°C)	10

PART 4

RESULTS

In this chapter, the data and operating conditions of the White Cement Plant in Fallujah were used in the thermodynamics analysis for the different types of cogeneration system. The results were obtained by using the Engineering Equation Solver program (EES). The main parameters of pre-heating gases are listed in Table 4.1.

Table 4.1. Main parameters of pre-heating at the Fallujah White Cement Plant.

Parameters	Quantity	Units
Gas flow	321000	Nm ³ /h
Temperature	380	°C
N ₂ gas	62%	
Dust content	85	g/Nm ³
CO ₂ gas	26.2%	
O ₂ gas	4.4%	
H ₂ O	7.4%	

The conditions of exhaust gas are summarized in Table 4.2. lists the main assumptions for the calculations of the generation systems.

Table 4.2. Conditions of exhaust gases for the Fallujah cement plant.

Outlet Temperature of preheater (°C)	380
Outlet Temperature of SP Boiler (°C)	225
Outlet Temperature of clinker cooler (°C)	350
Outlet mass flow-rate of preheater (kg/s)	113.46
Outlet mass flow-rate of clinker cooler (kg/s)	82.74

Table 4.3. Main assumptions for the system.

Isentropic Efficiency of Turbines (%)	85
Pressure of Environment (MPa)	0.10135
Temperature of Environment (°C)	25
Isentropic Efficiency of Pump (%)	70
Turbine Exhaust Dryness Percentage (%)	88
Temperature Difference at an Approach Point (°C)	5
Temperature Difference at a Pinch Point (°C)	10

The organic Rankine cycle analysis results are summarized in Tables 4.4 and 4.5. Figure 4.1 presents the T- s diagram for the organic Rankine cycle. The results show that the power produced from the ORC is 9509 kW, and the thermal efficiency reaches 21.42%. The thermodynamics properties for each state of the ORC system are listed in Table 4.11. The main results of the exergy analysis are listed in Table 4.6. The results also reveal that 65.46% of the total incoming exergy is lost during the condensation process, followed by losses in the exergy in the SP and AQC boilers of 16.83% and 11.88%, respectively. Finally, the exergy losses in the rest of the equipments are estimated to be 36.75% of the total exergy inputs. The exergy losses for each component of the ORC are presented in Figure 4.2.

Table 4.4. ORC Performance.

Work of turbine	9951 kW
Work of pump	441.5 kW
Exhaust temperature of AQC boiler	70°C
Heat input of AQC boiler	23320 kW
Heat input of SP boiler	21084 kW
Total heat input	44404 kW
Net output power	9509 kW
Exergy efficiency	34.52%
Thermal efficiency	21.42%

Table 4.5. The properties for each state for the organic Rankine cycle.

State	\dot{m} (kg/s)	P (MPa)	T (°C)	h (kJ/kg)	S (kJ/Kg.K)	EX (kW)	V (m ³ /kg)	x
1	62.19	3.5	250	563.1	1.895	6045		
2	62.19	3.5	21.84	224.1	1.077	144.3		
3	71.19	3.5	240	551.7	1.874	6567		
4	71.19	3.5	21.84	224.1	1.077	165.2		
5	133.4	3.5	21.84	224.1	1.077	309.5		
6	133.4	0.075	19.75	220.8	1.073	1.685	0.000732	0
7	133.4	0.075	134.6	482.4	1.916	1362		
8	133.4	3.5	244.6	557	1.884	12610		

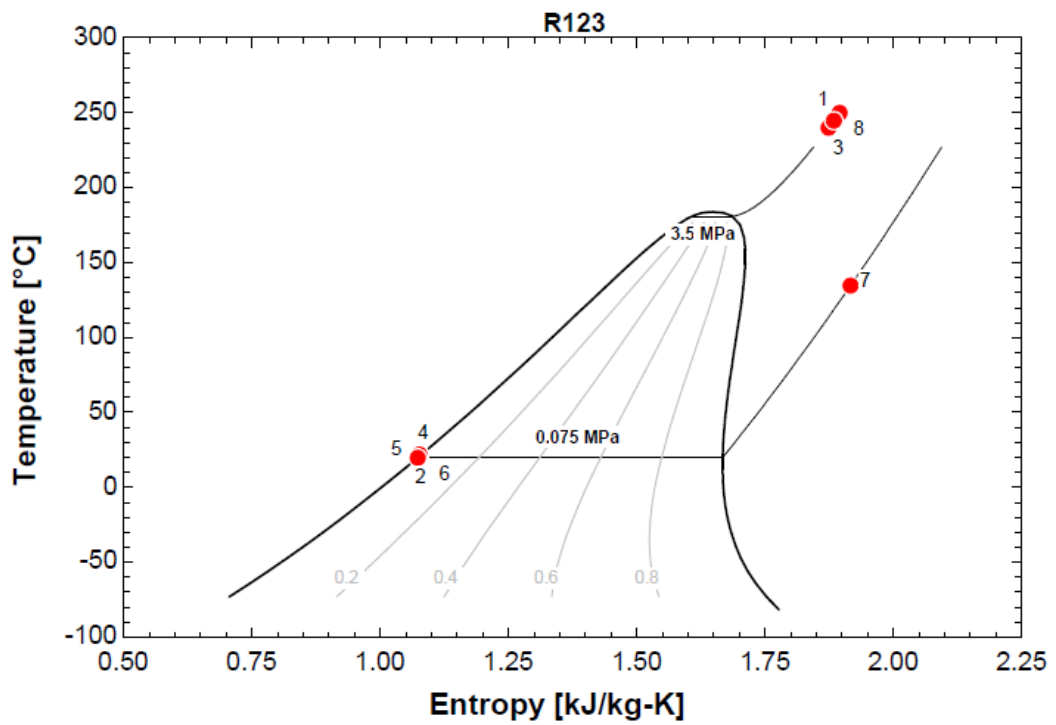


Figure 4.1. The (T-S) diagram for ORC.

Table 4.6. ORC exergy input, output and losses.

Exergy	State	Values (kW)	Percentage (%)
Input	AQC boiler	10191	37.0
	SP boiler	17357	63.0
	SUM	27548	100.0
Output	Net power	9509	34.51
Losses	AQC boiler	3275	11.88
	SP boiler	4637	16.83
	Turbine	1297	4.707
	Condenser	1361	4.939
	Pump	133.7	0.4852
	Mixture	2.198	0.007977
	AQC boiler exhaust	514.1	1.866
	SP boiler exhaust	6819	24.75

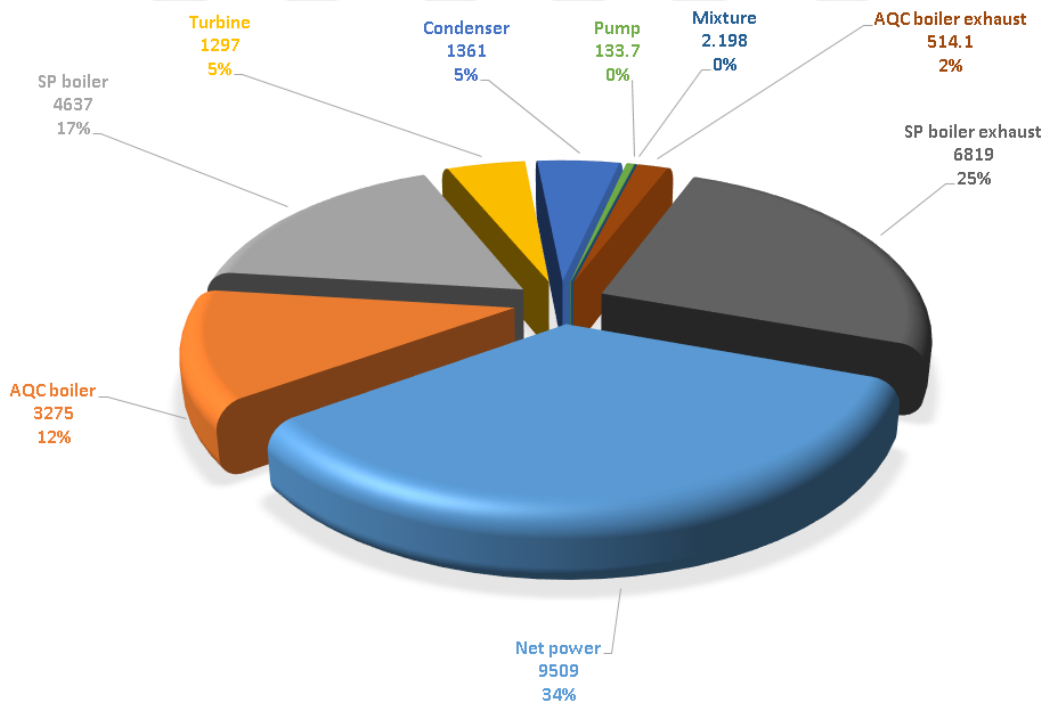


Figure 4.2. Exergy loss given exergy input percentages by ORC.

Analysis results for the single flash cycle regarding point and performance are summarize, as shown in Tables 4.7 and 4.8. Figure 4.3 shows the T- s diagram for the single flash steam cycle. The results show that the power produced from a single flash cycle is 12806 kW, and the thermal efficiency reaches 29.97%. Data from an analysis of the system is presented in Table 4.9 to find the wastage value in exergy. It was found that the losses amounted to 51.61%. These losses are distributed as follows: 24.75% are in the SP boiler exhaust, 1.866% in the AQC boiler exhaust, and 12.163% for the remaining components of the system. The heat added to the SP and AQC boilers caused exergy losses of 6.161% and 6.67%, respectively. Figure 4.4 shows the exergy losses for each component of a single flash cycle.

Table 4.7. Single flash cycle performance.

Work of turbine1	4018 kW
Work of turbine2	8830 kW
Work of pump 1	10.11 kW
Work of pump 2	33.26 kW
Exhaust temperature of AQC boiler	95°C
Heat input of AQC boiler	21644 kW
Heat input of SP boiler	21084 kW
Total heat input	42724 kW
Net output power	12806 kW
Exergy efficiency	46.48%
Thermal efficiency	29.97%

Table 4.8. The properties for each state for the single flash steam cycle.

State	m (kg/s)	P (MPa)	T (°C)	h (kJ/kg)	S (kJ/Kg.K)	EX (Kw)	V (m ³ /kg)	x
0		0.101	25	104.8	0.3669			
1	9.054	2	370	3,181	7.026	10,489		
2	9.054	2	200	852.6	2.33	1,651		
3	4.481	2	350	3,137	6.956	5,082		
4	20.3	2	69.03	290.6	0.9419	408.4		
5	6.768	2	200	852.6	2.33	1,234		
6	6.086	0.5	151.9	640.4	1.861	640.5	0.000732	
7	0.6811	0.5	151.9	2,749	6.821	534.6		
8	20.3	0.5	68.93	288.9	0.9416	377		
9	14.22	0.5	32.94	138.4	0.4768	27.72		
10	14.22	0.005	32.88	137.7	0.4761	20.47	0.001005	
11	13.54	2	363.4	3,166	7.003	15,570		
12	14.22	0.005	32.88	2,259	7.407	1,797		0.8757
13	6.765	0.5	151.8	852.5	2.36	1174		0.1007
14	15.82	2	200	852.5	2.33	2883		
15	13.53	0.5	206.8	2870	7.092	11215		
16	14.21	0.5	204.1	2865	7.079	11183		

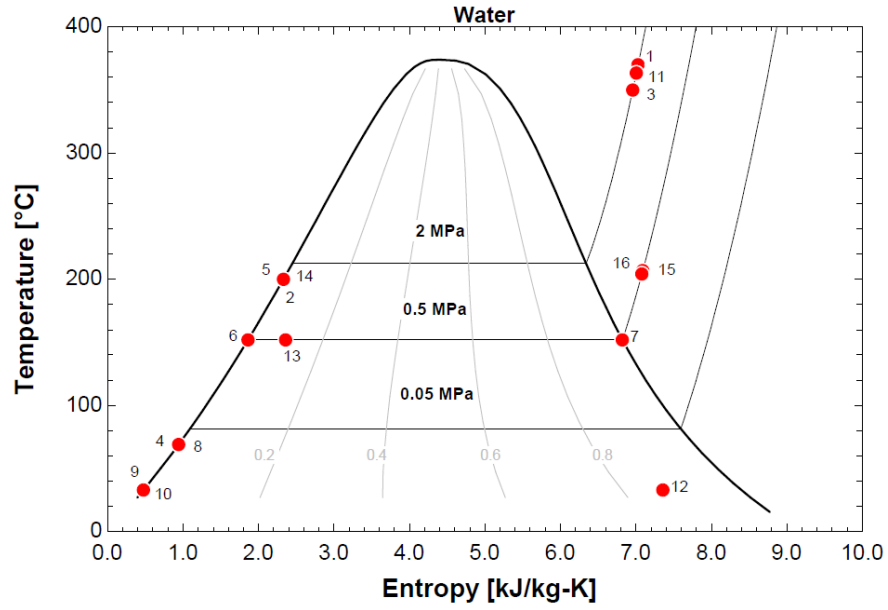


Figure 4.3. The (T-S) diagram for single flash cycle.

Table 4.9. Signal flash cycle exergy input, output, and losses.

Exergy	State	Values (kW)	Percentage (%)
Input	AQC boiler	10191	37.0
	SP boiler	17357	63.0
	SUM	27548	100.0
Output	Net power	12806	46.84
Losses	AQC boiler	1841	6.67
	SP boiler	1701	6.161
	Turbine 1	335.4	1.215
	Turbine 2	569.9	2.064
	Condenser	1762	6.384
	Pump 1	2.853	0.01033
	Flasher	58.97	0.2136
	Mixture 1	0.9564	0.003458
	Pump 2	1.819	0.006588
	Mixture 2	290.8	1.053
	Valve	58.97	0.2136
	AQC boiler exhaust	791.7	2.87
	SP boiler exhaust	6819	24.75

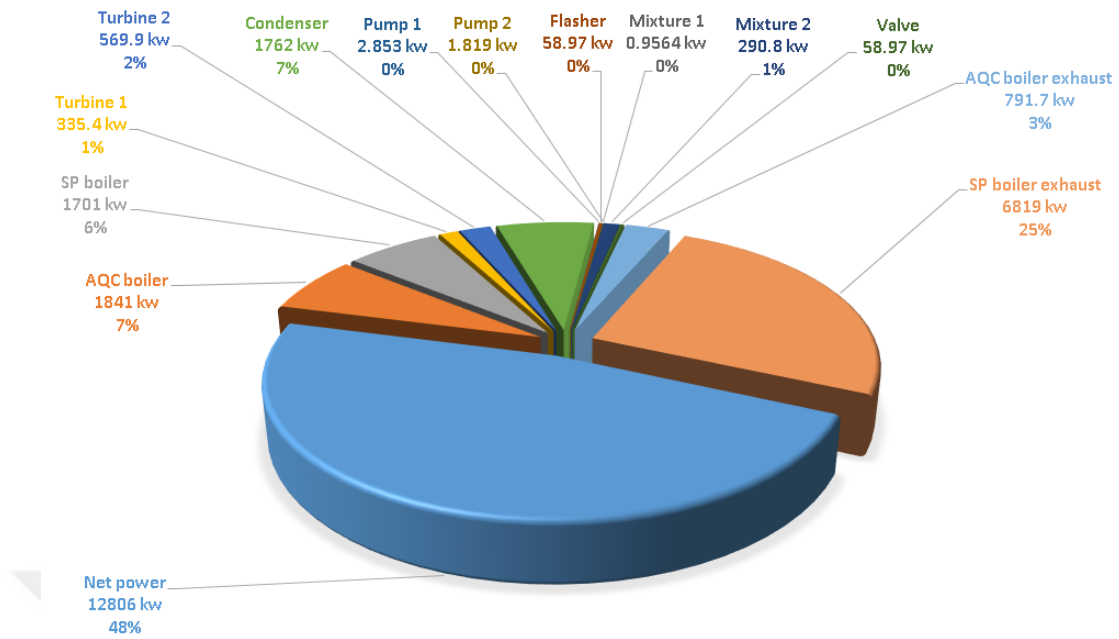


Figure 4.4. Exergy loss given exergy input percentages by single flash cycle.

The double-pressure steam cycle analysis results are summarized in Tables 4.10 and 4.11. Figure 4.5 presents the T- s diagram for double-pressure steam cycle. The results show that the power produced from the double-pressure steam cycles is 14095 kW, and the thermal efficiency reaches 33.18%. Table 4.12 presents the thermodynamics properties for each state of the system. Table 4.6 shows the exergy analysis of the double-pressure steam. The study found that 47.99% of the total incoming exergy is lost during the processes. These losses were distributed as follows: 25.1% in the SP boiler exhaust type, 3.092% in the AQC boiler exhaust type, and 19.81% in the rest of the components. Figure 4.6 presents the exergy loss for each component of a double-pressure steam cycle.

Table 4.10. Dual-Pressure steam performance.

Work of turbine 1	4909 kW
Work of turbine 2	9285 kW
Work of pump 1	16.51 kW
Work of pump 2	58.08 kW
Work of pump 3	24.13 kW
Exhaust temperature of AQC boiler	98°C
Heat input of AQC boiler	21392 kW
Heat input of SP boiler	21084 kW
Total Heat input	42476 kW
Net output power	14095 kW
Exergy efficiency	51.17%
Thermal efficiency	33.18%

Table 4.11. The properties for each state for the dual-pressure steam cycle.

State	m (Kg/s)	P (MPa)	T (°C)	S (kJ/Kg.K)	h (kJ/kg)	EX (kW)	V (m ³ /kg)	x
0		0.101	25	0.2242	63.01			
1	8.743	5	370	6.531	3,120	10296		
2	8.743	5	167	2.007	708.5	998.4		
3	5.18	5	340	6.404	3041	5884		
4	5.18	5	166.5	2.003	706.5	588.2		
5	0.547	0.8	189	6.761	2813	438.9		
6	0.547	0.8	166	2.003	701.8	59.56		
7	8.743	0.8	166	2.003	701.8	952.1	0.001109	
8	5.18	0.8	166	2.003	701.8	564.1	0.001109	
9	14.47	0.8	32.98	0.4772	138.9	6.654		
10	14.47	0.005	32.88	0.4761	137.7	5.039	0.001005	
11	14.47	0.005	32.88	7.451	2272	805.5		0.8099
12	13.92	5	358.6	6.485	3092	16177		
13	13.92	0.8	170.4	6.596	2739	10820		
14	14.46	0.8	170.4	6.603	2742	11257		

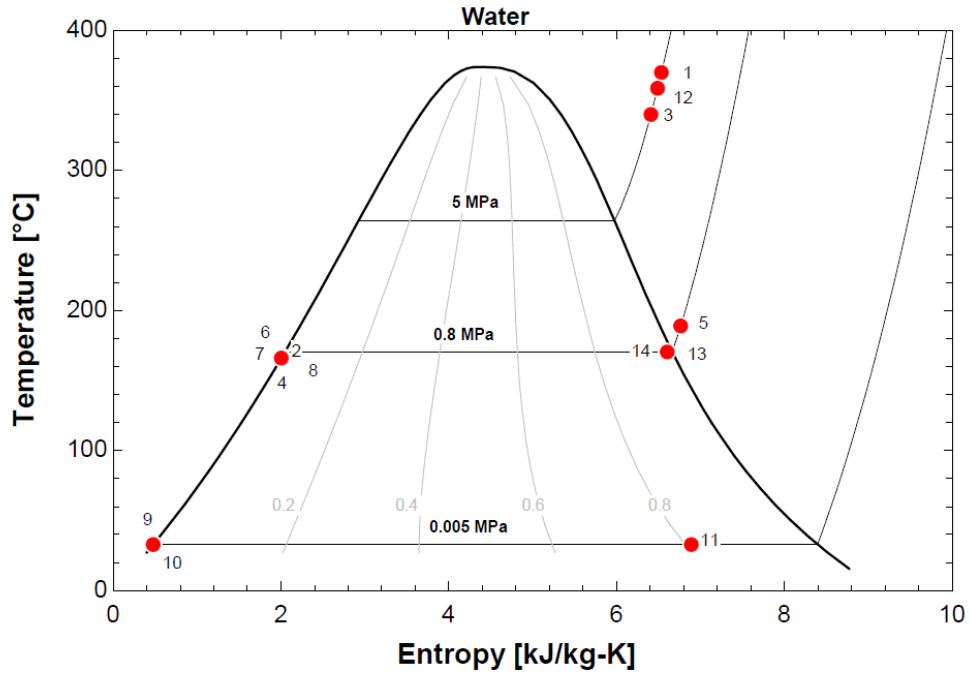


Figure 4.5. The (T-S) diagram for Dual-pressure steam cycle.

Table 4.12. Dual-pressure steam exergy input, output, and losses.

Exergy	State	Values (kW)	Percentage (%)
Input	AQC boiler	10191	37.0
	SP boiler	17357	63.0
	SUM	27548	100.0
Output	Net power	14095	51.16
Losses	AQC boiler	1522	5.614
	SP boiler	1242	4.579
	Turbine 1	449.7	1.695
	Turbine 2	269.1	0.9925
	Condenser	1697	6.259
	Mixer 1	2.912	0.01074
	Mixer 2	150.4	0.5546
	Pump 1	15.75	0.05807
	Pump 2	11.81	0.04353
	Pump 3	0.01942	0.00007163
	AQC boiler exhaust	839.9	3.092
	SP boiler exhaust	6819	25.1

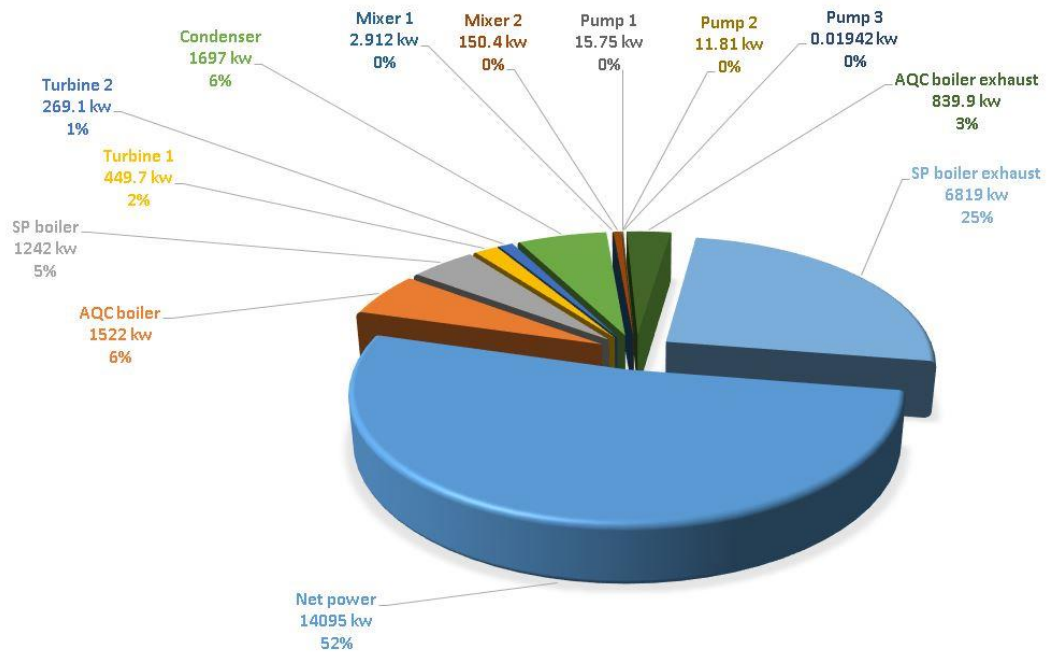


Figure 4.6. Exergy loss given exergy input percentages via dual steam cycle.

Table 4.13 shows the results obtained from the different cogeneration systems. The single flash cycle achieved the highest performance of power output and efficiencies (thermal and exergy). The lowest performance was obtained from the organic Rankine cycle.

Table 4.13. Results of improvement for various cogeneration systems.

Results	Orc Cycle	Single Flash Steam Cycle	Dual-Pressure Steam Cycle
Net output power	9509 kW	12806 kW	14095 kW
Exergy efficiency	34.52%	46.48%	51.17%
Thermal efficiency	21.42%	29.97%	33.18%

PART 5

CONCLUSION AND RECOMMENDATIONS

5.1. CONCLUSION

This study concludes that it is possible to work on the waste heat recovery project from the clinker grid cooler and the reheating tower without affecting the production process in the cement factory. It is better to focus on the waste heat from the AQC clinker cooler because it is completely released into the environment without benefiting from it, unlike the heat from the reheating tower. Part of this heat is used to heat raw materials before entering the rotary kiln so that the project does not affect production conditions. Each cogeneration cycle used in this study is a powerful and reliable tool in evaluating the best performance of each generation plant. The main conclusions of this study can be summarized as follows:

1. Reducing exergy losses in the AQC and SP boilers improved the performance of the cogeneration system.
2. Exergy analysis is the best design and performance evaluation tool in cogeneration systems, especially in energy-related systems.
3. In the cement factory, the Dual pressure steam cycle was the best performer compared to the other cycles used in the same factory regarding the power output and efficiency in contrast to the minor performance for the organic Rankine cycle under the same working conditions.
4. The organic Rankine cycle produced 9509 kW, and its thermal and exergy efficiencies were 21.42% and 34.52%, respectively.
5. The single flash steam cycle produced 12806 kW, and its thermal and exergy efficiencies were 29.97% and 46.48%, respectively.
6. The dual-pressure steam cycle produced 14095 kW, and its thermal and exergy efficiencies were 33.18% and 51.17%, respectively.

7. The results showed that the maximum exergy losses occur in the SP boiler for each cycle.

5.2. RECOMMENDATIONS

Through this study conducted on the waste heat recovery project in the cement factory, some important points that were not addressed in the previous literature or this thesis emerged, and they are related to this study and can be worked on in the future. It is possible to design a coil from the tubes and surround the rotary kiln in the firehouse area because the kiln crust temperature ranges between 200°C and 250°C, especially the area near the burner of the oven, called the firehouse. The heat would be transferred to the pipes by radiation and thermal oil that passes through these tubes and the oil would be heated. Then this oil would be transferred to a heat exchanger to heat the black oil used as fuel for furnaces or to heat water for heating purposes for buildings or other uses. Here, the heat of the kiln crust could be removed without using cooling fans or consuming electricity.

REFERENCES

1. Ayu, T. T., Hailu, M. H., Hagos, F. Y., & Atnaw, S. M., "Energy audit and waste heat recovery system design for a cement rotary kiln in Ethiopia: A case study", *International Journal of Automotive and Mechanical Engineering*, 1(2): 29-83 (2015).
2. Csernyei, C. M., "Numerical Modelling of a Rotary Cement Kiln with External Shell Cooling Fans", *Master Thesis, University of Western Ontario*, Canada, 34-45 (2016).
3. Fierro, J. J., Escudero-Atehortua, A., Nieto-Londoño, C., Giraldo, M., Jouhara, H., & Wrobel, L. C., "Evaluation of waste heat recovery technologies for the cement industry", *International Journal of Thermofluids*, 7(2): 100-400 (2020).
4. Hwan, I. H., "Heat transfer mechanisms in an indirectly heated rotary kiln with lifters and its role in scaling", *Doctoral Dissertation, Curtin University*, Australia, 21-33 (2009).
5. Amiri, A., & Vaseghi, M. R., "Waste heat recovery power generation systems for cement production process", *Transactions on Industry Applications*, 51(1): 13-19 (2014).
6. Wiederkehr, T. H., "Power generation by waste heat recovery", *Cement Symposium*, 1(3): 59-66 (1985).
7. Szabó, L., Hidalgo, I., Císcar, J. C., Soria, A., & Russ, P., "Energy consumption and CO2 emissions from the world cement industry", *European Commission Joint Research Centre, Report EUR*, 20(7): 6-9 (2003).
8. Gorbatenko, Y., Hedman, B. A., Shah, J. V., & Sharabaroff, A., "Waste heat recovery for the cement sector: market and supplier analysis", *The World Bank, USA*, 1-90 (2014).
9. International Finance Corporation, "Improving Thermal and Electric Energy Efficiency at Cement Plants: International Best Practice", *World Bank, USA*, 67-89 (2017).
10. Fog, M. H., & Nadkarni, K. L., "Energy efficiency and fuel substitution in the cement industry with E phas is on developing countries", *The world Bank, USA*, 23-31 (1983).

11. Ke, J., Price, L., McNeil, M., Khanna, N. Z., & Zhou, N., "Analysis and practices of energy benchmarking for industry from the perspective of systems engineering", *Energy*, 5(4): 32-44 (2013).
12. Njoku, O., Bafuwa, R., Mgbemene, C. & Ekechukwu, V., "Benchmarking energy utilization in cement manufacturing processes in Nigeria and estimation of savings opportunities", *Clean Technologies and Environmental Policy*, 19(6): 1639-1653 (2017).
13. Saunders, A., & Magazine, G. C., "Top 75 global cement companies", *Global Cement Magazine*, 2(3): 3-4 (2013).
14. Shrouf, F., Ordieres, J., & Miragliotta, G., "Smart factories in Industry 4.0: A review of the concept and of energy management approached in production based on the Internet of Things paradigm", *International Conference on Industrial Engineering and Engineering Management*, Australia, 697-701 (2014).
15. Brown, M. A., & Wang, Y., "Green savings: how policies and markets drive energy efficiency: how policies and markets drive energy efficiency", *ABC-CLIO*, California, USA, 56-64 (2015).
16. Doe, U., "An assessment of energy technologies and research opportunities", *Quadrennial Technology Review. United States Department of Energy*, USA, 12-19 (2015).
17. Forman, C., Muritala, I. K., Pardemann, R., & Meyer, B., "Estimating the global waste heat potential", *Renewable and Sustainable Energy Reviews*, 5(7): 1568-1579 (2016).
18. Smidth, F. L., "Preheater calciner systems", *FLSmidth*, Denmark, 45-57, (2011).
19. Ponssard, J. P., & Walker, N., "EU emissions trading and the cement sector: a spatial competition analysis", *Climate Policy*, 8(5): 467-493 (2008).
20. Απέργη, Π., "Power generation from waste heat in cement plants: application in Lafarge Volos plant", *Master's Thesis, University of Thessaly*, Greece, 34-67 (2012).
21. Terblanche, U., "Effective use of excess heat in a cement plant", *Master of Science Thesis, KTH School of Industrial Engineering and Management*, Denmark, 45-57 (2012).
22. Industry, I. C. Existing and Potential Technologies for Carbon Emissions Reductions in the Indian Cement Industry, *Indian Cement Industry*, India, 67-78 (2013)
23. Sztékler, K., Wojciechowski, K., Komorowski, M., & Tarnowska, M., "The thermoelectric generators use for waste heat utilization from cement plant", *EDP Sciences*, 1(4):10-31(2017).

24. Internet: Mohammed, S., & Bawazir R., "Waste Heat Recovery System (Whrs) for Cement Industry-a Casestudy for Hadhramout Cement Factory, Arabian Yemen Cement Company Limited (Ayccl)-Mukalla-Hadhramout," <http://nccyemen.com/en/pdf/fptcc.pdf?wmode=transparent/>(2019).
25. Karellas, S., Leontaritis, A. D., Panousis, G., Bellos, E., & Kakaras, E., "Energetic and exergetic analysis of waste heat recovery systems in the cement industry", *Energy*, 5(8): 147-156 (2013).
26. Arrieta, M. D. P., & Arrieta, F. R. P., "KCS34 evaluation for WHR in cement industry", *International Journal of Advanced Engineering Research and Science*, 5(11): 245-268 (2018).
27. Elson, A., Tidball, R., & Hampson, A., "Waste heat to power market assessment", *Building Technologies Research and Integration Center (BTRIC), Oak Ridge National Laboratory (ORNL), USA*, 24-28 (2015).
28. Riyanto, H., & Martowibowo, S. Y., "Optimization of Organic Rankine Cycle Waste Heat Recovery for Power Generation in a Cement Plant via Response Surface Methodology", *International Journal of Technology*, 6(6): 938-945 (2015).
29. Radwan, A. M., "Different possible ways for saving energy in the cement production", *Advances in Applied Science Research*, 3(2): 1162-1174 (2012).
30. Jenkins, B., & Mullinger, P., "Industrial and process furnaces: principles, design and operation", *Elsevier*, Germany, 45-53 (2011).
31. Favier, A., De Wolf, C., Scrivener, K., & Habert, G., "A sustainable future for the European Cement and Concrete Industry: Technology assessment for full decarbonization of the industry by 2050", *Technology assessment for full decarbonisation of the industry by 2050*, Zurich, 12-19 (2018).
32. Al-Rawashdeh, H. A., Gomaa, M. R., Mustafa, R. J., & Hasan, A. O., "Efficiency and Exergy Enhancement of ORC Powered by Recovering Flue Gases-Heat System in Cement Industrials: A Case Study", *Int. Rev. Mech. Eng*, 1(3): 185-197 (2019).
33. Yan, Q., Zhou, C. B., Qu, P., & Zhang, R. Q., "The promotion of clean development mechanism to cement industry capturing waste heat for power generation in China", *Mitigation and Adaptation Strategies for Global Change*, 14(8): 793-804 (2009).
34. Zeman, F., "Oxygen combustion in cement production", *Energy Procedia*, 1(1): 187-194 (2009).
35. Söğüt, Z., Oktay, Z., & Karakoç, H., "Mathematical modeling of heat recovery from a rotary kiln", *Applied Thermal Engineering*, 30(9): 817-825 (2010).

36. Mikulčić, H., Vujanović, M., & Duić, N., "Reducing the CO₂ emissions in Croatian cement industry", *Applied Energy*, 10(1): 41-48. (2013).
37. Brunke, J. C., & Blesl, M., "Energy conservation measures for the German cement industry and their ability to compensate for rising energy-related production costs", *Journal of Cleaner Production*, 8(2): 94-111 (2014).
38. Luo, Q., Li, P., Cai, L., Zhou, P., Tang, D., Zhai, P., & Zhang, Q., "A thermoelectric waste-heat-recovery system for portland cement rotary kilns", *Journal of Electronic Materials*, 44(6): 1750-1762 (2015).
39. Guo, C., Du, X., Yang, L., & Yang, Y., "Organic Rankine cycle for power recovery of exhaust flue gas", *Applied Thermal Engineering*, 7(5): 135-144 (2015).
40. Amini, A., Mirkhani, N., Pourfard, P. P., Ashjaee, M., & Khodkar, M. A., "Thermo-economic optimization of low-grade waste heat recovery in Yazd combined-cycle power plant (Iran) by a CO₂ transcritical Rankine cycle", *Energy*, 8(6): 74-84 (2015).
41. Maalouf, S., Ksayer, E. B., & Clodic, D., "Investigation of direct contact condensation for wet flue-gas waste heat recovery using Organic Rankine Cycle", *Energy Conversion and Management*, 10(7): 96-102 (2016).
42. Huang, Y. H., Chang, Y. L., & Fleiter, T., "A critical analysis of energy efficiency improvement potentials in Taiwan's cement industry", *Energy Policy*, 9(6): 14-26 (2016).
43. Boldyryev, S., "Heat Integration in a Cement Production", *In Cement Based Materials*, United Kingdom, 23-34 (2018).
44. Ahmed, A., Esmail, K. K., Irfan, M. A., & Al-Mufadi, F. A., "Design methodology of organic Rankine cycle for waste heat recovery in cement plants", *Applied Thermal Engineering*, 12(9): 421-430 (2018).
45. Koroneos, C., Roumbas, G., & Moussiopoulos, N., "Exergy analysis of cement production", *International Journal of Exergy*, 2(1): 55-68 (2005).
46. Naeimi, A., Bidi, M., Ahmadi, M. H., Kumar, R., Sadeghzadeh, M., & Nazari, M. A., "Design and exergy analysis of waste heat recovery system and gas engine for power generation in Tehran cement factory", *Thermal Science and Engineering Progress*, 9(2): 299-307 (2019).
47. Moreira, L. F., & Arrieta, F. R. P., "Thermal and economic assessment of organic Rankine cycles for waste heat recovery in cement plants", *Renewable and Sustainable Energy Reviews*, 11(4): 109315 (2019).
48. Mirhosseini, M., Rezania, A., & Rosendahl, L., "Power optimization and economic evaluation of thermoelectric waste heat recovery system around a rotary cement kiln", *Journal of Cleaner Production*, 23(2): 1321-1334 (2019).

49. Júnior, E. P. B., Arrieta, M. D. P., Arrieta, F. R. P., & Silva, C. H. F., "Assessment of a Kalina cycle for waste heat recovery in the cement industry", *Applied Thermal Engineering*, 14(7): 421-437 (2019).
50. Zhao, Y., & Wang, J., "Exergoeconomic analysis and optimization of a flash-binary geothermal power system", *Applied Energy*, 17(9): 159-170 (2016).
51. Castelli, M. R., Englaro, A., & Benini, E., "The Darrieus wind turbine: Proposal for a new performance prediction model based on CFD", *Energy*, 36(8): 4919-4934 (2011).
52. Wang, J., Dai, Y., & Gao, L., "Exergy analyses and parametric optimizations for different cogeneration power plants in cement industry", *Applied Energy*, 86(6): 941-948 (2009).
53. Behzadi, A., Gholamian, E., Houshfar, E., & Habibollahzade, A., "Multi-objective optimization and exergoeconomic analysis of waste heat recovery from Tehran's waste-to-energy plant integrated with an ORC unit", *Energy*, 1(60): 1055-1068 (2018).
54. Kuo, C. H., Pei, B. S., & Tsai, K. F., "A study of organic working fluids on system efficiency of an ORC using low-grade energy sources", *Energy*, 35(3): 1403-1411 (2010).
55. Wang, H., Xu, J., Yang, X., Miao, Z., & Yu, C., "Organic Rankine cycle saves energy and reduces gas emissions for cement production", *Energy*, 8(6): 59-73 (2015).
56. Pishkariahmadabad, M., Ayed, H., Xia, W. F., Aryanfar, Y., Almutlaq, A. M., & Bouallegue, B., "Case Studies in Thermal Engineering", Elsevier, 22(14): 45-57 (2021).
57. Internet: Science Direct, "Energy and exergy and economics analysis of a two stages organic", [https://doi.org/10.1016/j.csite.2021.101554/\(2021\)](https://doi.org/10.1016/j.csite.2021.101554/(2021)).
58. M. Cengel, Y. A., Boles, M. A., & Kanoglu, "Thermodynamics: an engineering approach", **McGraw-hill**, New York, 20-26 (2011).
59. Varma, G. P., & Srinivas, T., "Parametric analysis of steam flashing in a power plant using waste heat of cement factory", *Energy Procedia*, 9(10): 99-106 (2016).
60. Saleh, B., Koglbauer, G., Wendland, M., & Fischer, J., "Working fluids for low-temperature organic Rankine cycles", *Energy*, 32(7): 1210-1221 (2007).
61. A. Akroot, "Effect of Operating Temperatures on the Performance of a SOFCGT Hybrid System," *Int. J. Trend Sci. Res. Dev.*, 3(3): 1512–1515 (2019).

62. Martínez, E. H. Carlos, M. C. P. A. Solís, J. I. C. and Avalos, M. C. M. del C. P. “Thermodynamic simulation and mathematical model for single and double flash cycles of Cerro Prieto geothermal power plants,” *Geothermics*, 8(3): 101-713(2020).
63. Akroot, A. “Modelling of Thermal and Water Management in Automotive Polymer Electrolyte Membrane Fuel Cell Systems,” *Master Thesis, Hacettepe University*, Ankara, Turkey, 23-38 (2014).
64. Akroot, A. Namli, L. and Ozcan, H. “Compared Thermal Modeling of Anode- and Electrolyte-Supported SOFC-Gas Turbine Hybrid Systems,” *J. Electrochem. Energy Convers. Storage*, 18(1): 134-178 (2021).
65. Jalilinasrabad, S. Itoi, R. Valdimarsson, P. Saevarsdottir, G. and Fujii, H. “Flash cycle optimization of Sabalan geothermal power plant employing exergy concept,” *Geothermics*, 4(3): 75–82 (2012).

RESUME

Hussein Ali Mutlag Al-Mutlag graduated from primary, preparatory and secondary schools in that city. After that, he started his undergraduate program at the University of Technology in Baghdad, Department of Mechanical Engineering in 1996. He then worked as an engineer at the Fallujah Cement Factory in 2001, And continues in the same factory in the Chief Engineers position. In 2019, he started at Karabük University, Mechanical Engineering Department to complete his master's degree.